Glycoconjugate Journal
https://doi.org/10.1007/s10719-021-10017-9

ORIGINAL ARTICLE

Sialidase neu4 deficiency is associated with neuroinflammation in mice

Zehra Kevser Timur[1] · Orhan Kerim Inci[1] · Secil Akyildiz Demir[2] · Volkan Seyrantepe[1,2]

Received: 7 April 2021 / Revised: 11 July 2021 / Accepted: 12 August 2021

Abstract

Sialidases catalyze the removal of sialic acid residues from glycoproteins, oligosaccharides, and sialylated glycolipids. Sialidase Neu4 is in the lysosome and has broad substrate specificity. Previously generated *Neu4-/-* mice were viable, fertile and lacked gross morphological abnormalities, but displayed a marked vacuolization and lysosomal storage in lung and spleen cells. In addition, we showed that there is an increased level of GD1a ganglioside and a markedly decreased level of GM1 ganglioside in the brain of *Neu4-/-* mice. In this study, we further explored whether sialidase Neu4 deficiency causes neuroinflammation. We demostrated that elevated level of GD1a and GT1b is associated with an increased level of LAMP1-positive lysosomal vesicles and Tunel-positive neurons correlated with alterations in the expression of cytokines and chemokines in adult *Neu4-/-* mice. Astrogliosis and microgliosis were also significantly enhanced in the hippocampus, and cerebellum. These changes in brain immunity were accompanied by motor impairment in these mice. Our results indicate that sialidase Neu4 is a novel mediator of an inflammatory response in the mouse brain due to the altered catabolism of gangliosides.

Keywords Sialidase · Neu4 · Ganglioside · Neuroinflammation · Behavior

Introduction

Sialidases catalyze the removal of sialic acid residues from glycoproteins, oligosaccharides, and sialylated glycolipids. There are four genetically distinct sialidases that vary in subcellular location, tissue distribution and level of expression [1]. Neu1 is the lysosomal sialidase that is a component of the heterotrimeric complex with β-galactosidase (β-Gal) and cathepsin A (CathA) in lysosomes [2, 3]. Sialidase Neu1 localizes not only in lysosomes but also in cytoplasmic vesicles and the plasma membrane. Moreover, sialidase Neu1 is differentially expressed in various tissues and cell types such as the brain, liver, leukocytes and fibroblasts [4]. [Mutation of the Neu1 gene causes a type of severe lysosomal storage disease (LSD) referred to as sialidosis. Neu2 is a cytosolic sialidase that is expressed mostly in skeletal muscle and cleaves GM3 ganglioside to alter cytoskeletal structure [5–7]. Neu3 is a plasma membrane associated sialidase that is expressed mostly in the adrenal gland, heart, testis, skeletal muscle and thymus. Sialidase Neu3 is involved in intracellular signaling of neuritogenesis and apoptosis [8, 9]. Sialidase Neu4 is localized in the lysosomes, mitochondria and endoplasmic reticulum and has broad substrate specificity [10–12]. It catalyzes removal of sialic acids from glycoprotein, gangliosides and oligosaccharides as well as degradation of the sialic acid polymer.

The Neu4 gene encodes two isoforms both in humans and murine models. The Neu4a (murine) isoform includes an additional 23 aa sequence at the N terminus [13], but Neu4L (human) only contains an additional 12 aa sequence [12]. Morever, Neu4b is classified as a short form in the murine-like human Neu4S. These isoforms have vast substrate specificity for gangliosides and glycoproteins, as well as oligosaccharides alike [10]. Subcellular localization of these isoforms show that Neu4a and Neu4b isoforms partially localizes in the calnexin positive ER membranes [14, 15], however the locations differ between Neu4L and Neu4S. Neu4L localizes both in the mitochondria and lysosome, but Neu4S is found in the ER membranes [12]. Although Neu4a and Neu4b exhibit different enzymatic activity, the human isoforms elicit similar activity. Neu4a which is highly expressed in the brain,

✉ Volkan Seyrantepe
volkanseyrantepe@iyte.edu.tr

[1] Department of Molecular Biology and Genetics, Izmir Institute of Technology, Urla, Izmir, Turkey

[2] Izmir Institute of Technology, IYTEDEHAM, Urla, İzmir, Turkey

Published online: 23 October 2021

elicits low sialidase activity, Neu4b displays higher sialidase activity than the long isoform [12, 16]. Despite low sialidase activity for Neu4a, this isoform plays a crucial role in neural development and plasticity due to hydrolysis of neural cell adhesion molecule [17–19]. In addition, Neu4b overexpression causes suppression of neurite formation in Neuro2a cells after treatment with retinoic acid [13]. Apart from a neurodevelopmental role, human isoforms also play various biological roles in cancer [20, 21] and neuronal apoptosis [22].

We previously generated a mouse model with a deficiency in sialidase Neu4. *Neu4-/-* mice were viable, fertile and lacked gross morphological abnormalities, but showed a marked vacuolization and lysosomal storage especially in the lung and spleen tissues. We also have demonstrated an increased level of GD1a ganglioside and a markedly decreased level of GM1 ganglioside in brain tissue of *Neu4-/-* mice by thin layer chromatography analysis [23]. In an attempt to clarify the role of sialidase Neu4 in GM2 ganglioside degradation in a hexosaminidase A deficient Tay-Sachs disease mouse model (*Hexa-/-),* we generated double-knockout mice with combined deficiency in hexosaminidase A and sialidase Neu4. *Hexa-/-Neu4-/-* mice showed epileptic seizures with 40% penetrance correlating with polyspike discharges in the cortical electrodes of the electroencephalogram. We also demostrated that double knockouts have multiple degenerating neurons with increased levels of GM2 ganglioside. Based on these observations we suggested that sialidase Neu4 deficiency exacerbates the phenotype in the mouse model of Tay-Sachs disease indicating that sialidase Neu4 is a modifier gene, and its deficiency reduces the disease severity through the metabolic bypass [24].

Gangliosides, sialic acid-containing glycosphingolipids, are abundantly expressed in the nervous system. They are synthesized by glycosyltransferases and sialyltransferases in the Golgi apparatus [25]. GM1, GD1a, GD1b and GT1b are the complex gangliosides which comprise up to 97% of gangliosides in brain. It has been reported that ST3GAL2 (ST3 Beta-Galactoside Alpha-2,3-Sialyltransferase 2) and ST3GAL3 sialyltransferases are primarily responsible for ganglioside terminal *α2-3* sialylation in the brain, synthesizing GD1a and GT1b in the mouse [26]. Gangliosides mediate different biological processes such as proliferation, adhesion, cell differentiation, and inflammation [26–29]. Studies show that gangliosides cause inflammation via toll-like receptor (TLR) which is located in cell membrane as a sensor of various pathogens and trigger immune response [30, 31]. Moreover, Amith et al. showed that sialidase Neu1 activation mediate ligand-induced TLR responses against infectious diseases [32]. On the other hand, it has been reported that the accumulation of gangliosides in lysosomes leads to neuroinflammation in several LSDs that affect the central nervous systems [33]. Under normal conditions microglial cells stay in an inactive stage but the accumulated macromolecules activate microglial cells causing an increased inflammatory response indicating that inflammation has significant contribution to disease pathology [34]. Alterations in the inflammatory cytokine and chemokine genes expressions levels have been shown in mouse models of several LSDs. It has been reported that there is high expression of proinflammatory cytokines in the central and peripheral nervous system in mouse model of GM1 and GM2 gangliosidosis [35]. In contrast, low levels of GM1 ganglioside have been observed in various neurodegenerative disorders including Parkinson and Huntington diseases [36, 37]. Numerous studies have also demonstrated that GM1 ganglioside displays neuroprotective and anti-neurotoxic processes [38]. GM1 ganglioside in particular plays an essential role in reducing inflammation in Aβ-induced THP-1 cells. In addition, GM1 ganglioside treatment inhibits cytokine production via destabilization of Aβ aggregation [39]. Pan et al. recently demonstrated that combined deficiency of sialidase Neu3 and Neu4

Table 1 List of primers used for quantitative RT-PCR analysis

Gene Names	Forward primer	Reverse primer
Bcl-2	5'-CGCAGAGATGTCCAGTCAGC- 3'	5'-TATGCACCCAGAGTGATGCAG-3'
Bcl-xL	5'-TCAGCCACCATTGCTACCAG-3'	5'-GTCTGAGGCCACACACATCA-3'
Bax	5'-AGGATGCGTCCACCAAGAAG-3'	5'-CTTGGATCCAGACAA GCAGC-3'
ATF6	5'-TGGAAGTGGGAAGATCGGGA-3'	5'-AGGACAGAGAAACAAGCTCGG-3'
Calnexin	5'-ATTGCCAACCCCAAGTGTGA-3'	5'-TCCAGCATCTGCAGCACTAC-3'
SOD2	5'-GTGTCTGTGGGAGTCCAAGG-3'	5'-CCCCAGTCATAGTGCTGCAA-3'
Ccl2	5'-ATGCAGTTAATGCCCCACTC-3'	5'-TTCCTTATTGGGGTCAGCAC-3'
Ccl3	5'-TCTGTACCATGACACTCTGC-3'	5'-AATTGGCGTGGAATCTTCCG-3'
GFAP	5'-AGTAACATGCAAGAGACAGAG-3'	5'-TAGTCGTTAGCTTCGTGCTTG-3'
ST3Gal3	5'-CGCAAACTTTTCAGAGGGAG-3'	5'-AAGAGAGAATCGCGCTCGTA-3'
Neu1	5'-TCATCGCCATGAGGAGGTCCA-3'	5'-AAAGGGAATGCCGCTCACTCCA-3'
Neu2	5'-CGCAGAGTTGATTGTCCTGA-3'	5'-TTCTGAGCAGGGTGCAGTTTCC-3'
Neu3	5'-CTCAGTCAGAGATGAGGATGCT-3'	5'-GTGAGACATAGTAGGCATAGGC-3'
GAPDH	5'-CCCCTTCATTGACCTCAACTAC-3'	5'-ATGCATTGCTGACAATCTTGAG-3'

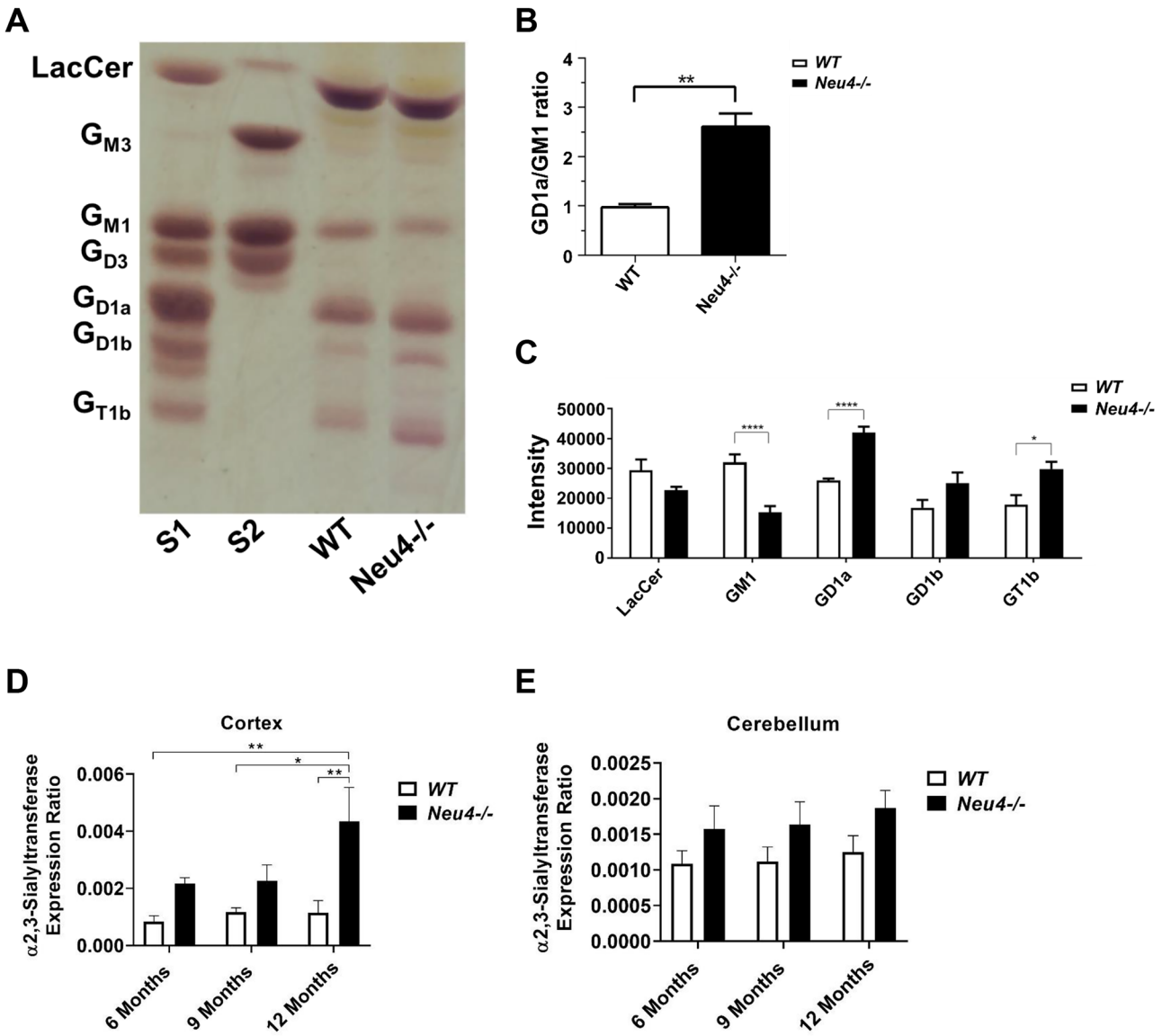

Fig. 1 Alterations of ganglioside profiles in the brain tissues of 9-month-old *Neu4-/-* and *WT* mice. Representative TLC image of orcinol-stained gangliosides from brain (Fig. S1, total ganglioside standard; Fig. S2, mixed ganglioside standard, GM3, GM1 and GD3) (**A**). Histogram displayed the ratio of GD1a/GM1 (**B**). Histogram shows the intensity of gangliosides (LacCer, GM1, GD1a, GD1b, GT1b) in 9-month-old *Neu4-/-* mice brain compared to age matched *WT* (**C**). Intensities were measured via ImageJ program. Relative mRNA expression levels of the α-2,3 sialyltransferase gene in the 6, 9 and 12-month-old *Neu4-/-* and *WT* mice cortex (**D**) and cerebellum (**E**). The data are represented as the mean ± SEM. Two-way ANOVA was used for statistical analysis (*$p < 0.05$, **$p < 0.025$, and ****$p < 0.001$)

in mice results in GM3 ganglioside accumulation and reduced levels of GM1 causing defects in neuritogenesis, accumulation of lipofuscin in neuron and memory loss [40].

In the present study, we aimed at gaining additional insight into the biological role of sialidase Neu4 by elucidating whether elevated GD1a/ GM1 ratio is associated with altered immune responses in sialidase Neu4 deficient adult mice (9-month-old) brain. In addition to quantitative RT-PCR and immunofluorescence methods, we included region-specific assessments of neuroinflammation and apoptosis in the brain, which is likely associated with impaired behaviors.

Materials and methods

Animals

Mice were bred in the animal core facility at IYTE. Animals were maintained at a constant temperature with an alternating 12-h light/dark cycle. Food and water were available ad libitum. All animal experiments were performed in accordance with the Turkish Institute of Animal Health guide for the care and use of laboratory animals. The animal

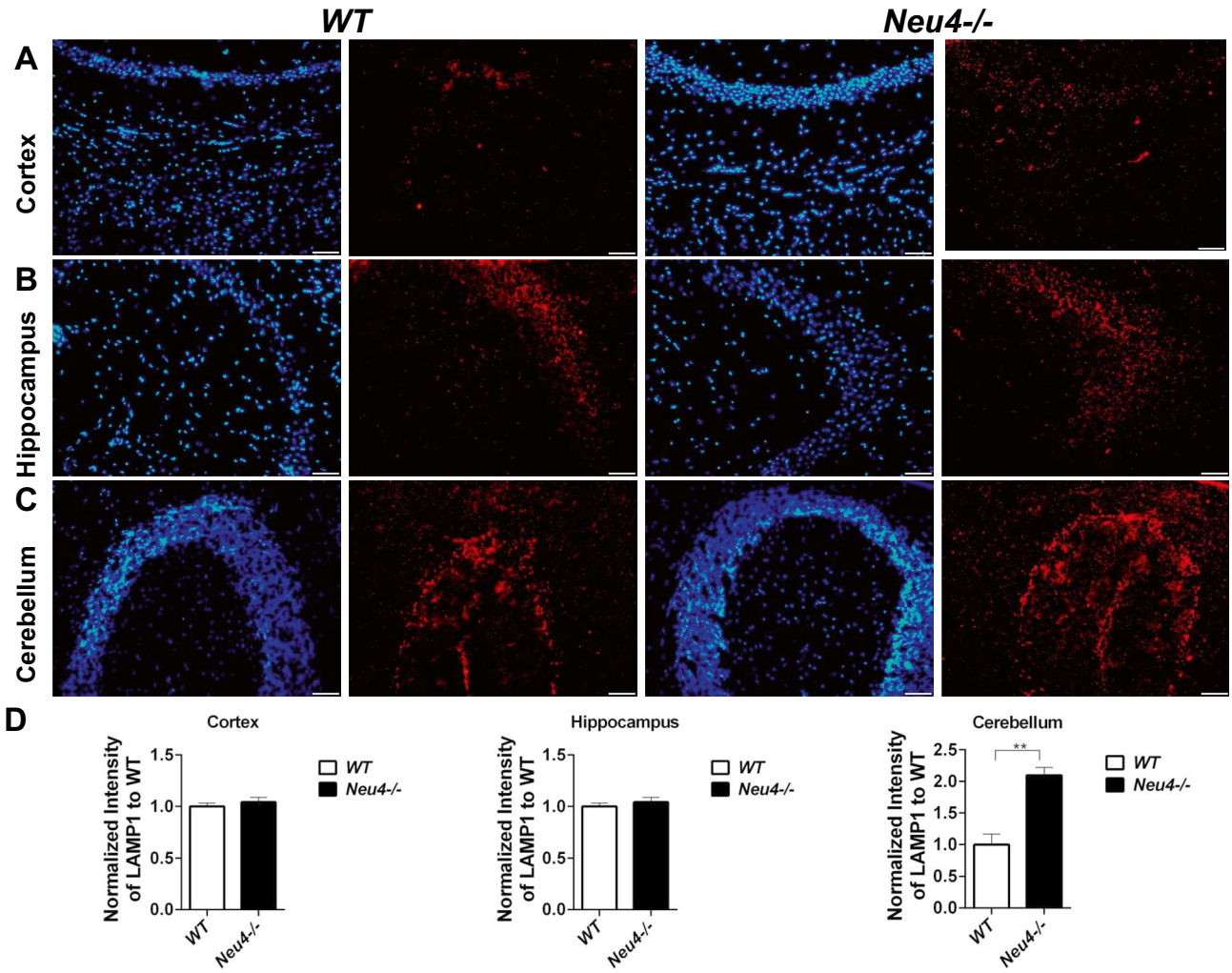

Fig. 2 Immunofluorescent staining of Lamp1 + cells in *Neu4-/-* mouse brain. Brain sections from cortex (**A**), hippocampus (**B**) and cerebellum (**C**) for 9-month-old *Neu4-/-* mouse compared with control were stained with anti-Lamp1 (red) and DAPI (blue) antibodies. Scale bar = 50 µm. Quantitative analysis (**D**) exhibits Lamp1 intensity that were detected by ImageJ. The data are represented as the mean ± SEM. Unpaired t-test was used for statistical analysis (**$p < 0.025$)

studies were approved by the Institutional Animal Care and Use Committee of the Izmir Institute of Technology. *WT* and *Neu4-/-* mice were sacrificed by cervical dislocation at 6, 9 and/or 12-month-old, their brain cortices and cerebellums were separated and immediately frozen by liquid nitrogen.

Thin layer chromatography analysis

Twenty-five mg of brain tissue from each mouse was homogenized in 2 ml of dH2O using the ultra turax homogenizer (IKA T10) for 30 s at 6000 rpm. The homogenized samples were sonicated (Bandelin-sonoplus) for 3 min. The samples were then dried with an N2 flow in the Reacti-Therm Heating module (Thermo) by 55 °C of water. The extraction was first performed with 3 ml of 100% acetone, to remove the supernatant. Then supernatants were collected via extraction with 1.5 ml of a chloroform:methanol:water (10:10:1) solution and, 2 ml of a chloroform:methanol:water (30:60:8) solution. In order to separate the acidic gangliosides, DEAE Sephadex A-25 was used. The DEAE Sephadex A-25 ion exchange columns were prepared freshly before usage [41]. The total ganglioside samples obtained were loaded in the columns, washed with 4 ml of 100% methanol, and then acidic gangliosides were eluted with 5 ml of 500 mM potassium acetate in methanol. A desalting process of the

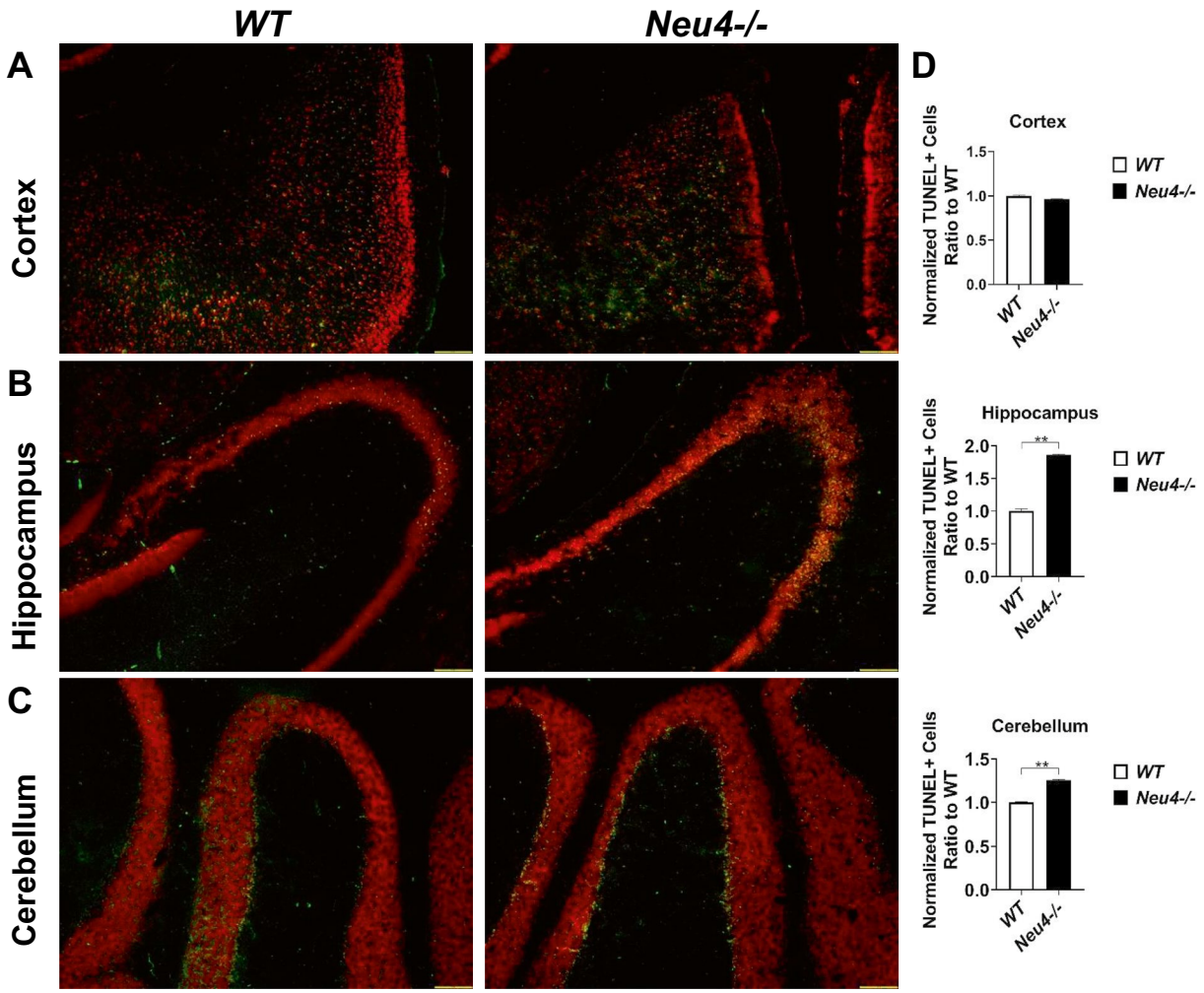

Fig. 3 Immunohistochemistry of the apoptotic cells by TUNEL assay in several brain regions. OCT-embedded sections from 9-month-old *Neu4-/-* mice cortex, hippocampus and cerebellum brain regions respectively were used for detection of apoptosis by TUNEL assay compared to age matched *WT* (**A**). Propidium Iodide (PI) represents cell nucleus staining. Scale bar = 50 µm. (**B**) Quantification of the fluorescence intensities in TUNEL assay were measured by selecting random fields. The data are represented as the mean ± SEM. Unpaired t-test was used for statistical analysis (**$p < 0.025$)

acidic gangliosides was carried out by the Supelclean LC-18 column (Supelco). The collected acidic gangliosides were loaded in the LC-18 columns, and the flow through was discarded. The columns were washed with 10 ml of distilled water and samples were eluted with 4 ml of methanol and 4 ml of chloroform:methanol (1:1) under low vacuum (< 5 Hg). The eluted samples were evaporated with an N2 flow. Samples were loaded onto silica plates (Merck) automatically (Linomat 5 Camag) and run in a chloroform:methanol: 0.2% CaCl2 (30:65:8) solution. Orcinol (Sigma) stain was prepared fresh before usage. For this 0.04 g orcinol was dissolved in 10 ml of 25% sulfuric acid. The plates were dyed with orcinol and incubated on a TLC plate heater (Camag) at 120 °C until all the bands became visible. After staining, the gangliosides were identified by a comparison with brain ganglioside standards (Avanti Polar Lipids). The plates were then scanned with the HP scanner system, and the band intensities were analyzed using the ImageJ program (Fiji).

For gene profiling with arrays, total RNA was extracted from cortical and cerebellar tissues from *WT* and *Neu4-/-* mice (n = 2) using an RNeasy Mini Kit (Qiagen, 74,134) following the manufacturer's instructions. cDNA was synthesized with an RT2 First Strand Kit (Qiagen, 330,401) following the manufacturer's instructions. Relative mRNA expressions of 84 key genes involved in the inflammation and cell signaling were determined using two different RT2 Profiler PCR Arrays (Qiagen, Mouse Cytokines & Chemokines, Cat. no. 330231 PAMM-150ZA, and Mouse Toll-Like Receptor Signaling Pathway PAMM-018ZA, respectively). Quantitative real-time PCRs were performed with a Roche Lightcycler 96 machine using RT2 Real-Time SYBR green PCR master mix (Qiagen,

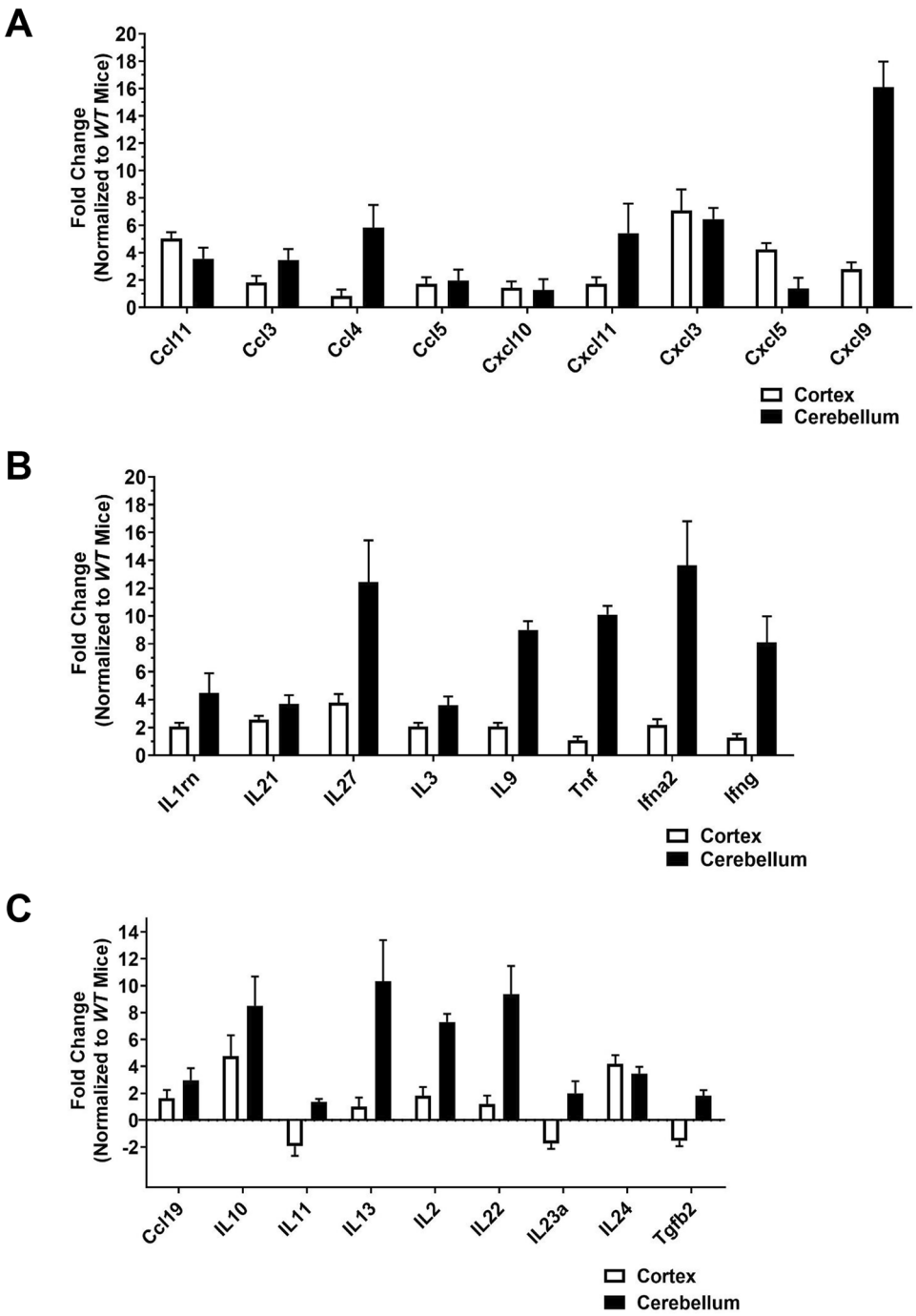

Fig. 4 Relative expression levels of pro-inflammatory chemokines (**A**), cytokines (**B**), and anti-inflammatory chemokine & cytokine genes (**C**), in 9-month-old *Neu4-/-* mice brain cortex (white bars) and cerebellum (black bars), normalized to *WT* mice (n = 2)

330,500) with an initial denaturation at 95 °C for 10 min, 45 cycles at 95 °C for 15 s, and 60 °C for 1 min. A signal was acquired at 60 °C during each cycle. Melting curve analysis was performed at the end of the reaction to verify PCR specificity. Each sample had a single peak in each reaction at a temperature greater than 80 °C which showed that there is no non-specific product. The threshold cycle changes (△Ct) denote the difference in Ct values for the gene of interest based on the Ct level of housekeeping genes. Expression of each gene was normalized using the mean expression of four different housekeeping genes in the array. Fold changes in the expression level of genes were obtained according to the $2-\Delta\Delta CT$ method. Differences among genotypes were analyzed by Student's t-test. Genes that had positive or negative fold changes of more than 1.5-fold with a p-value smaller than 0.05, were chosen for each array separately, graphed and considered as statistically significant.

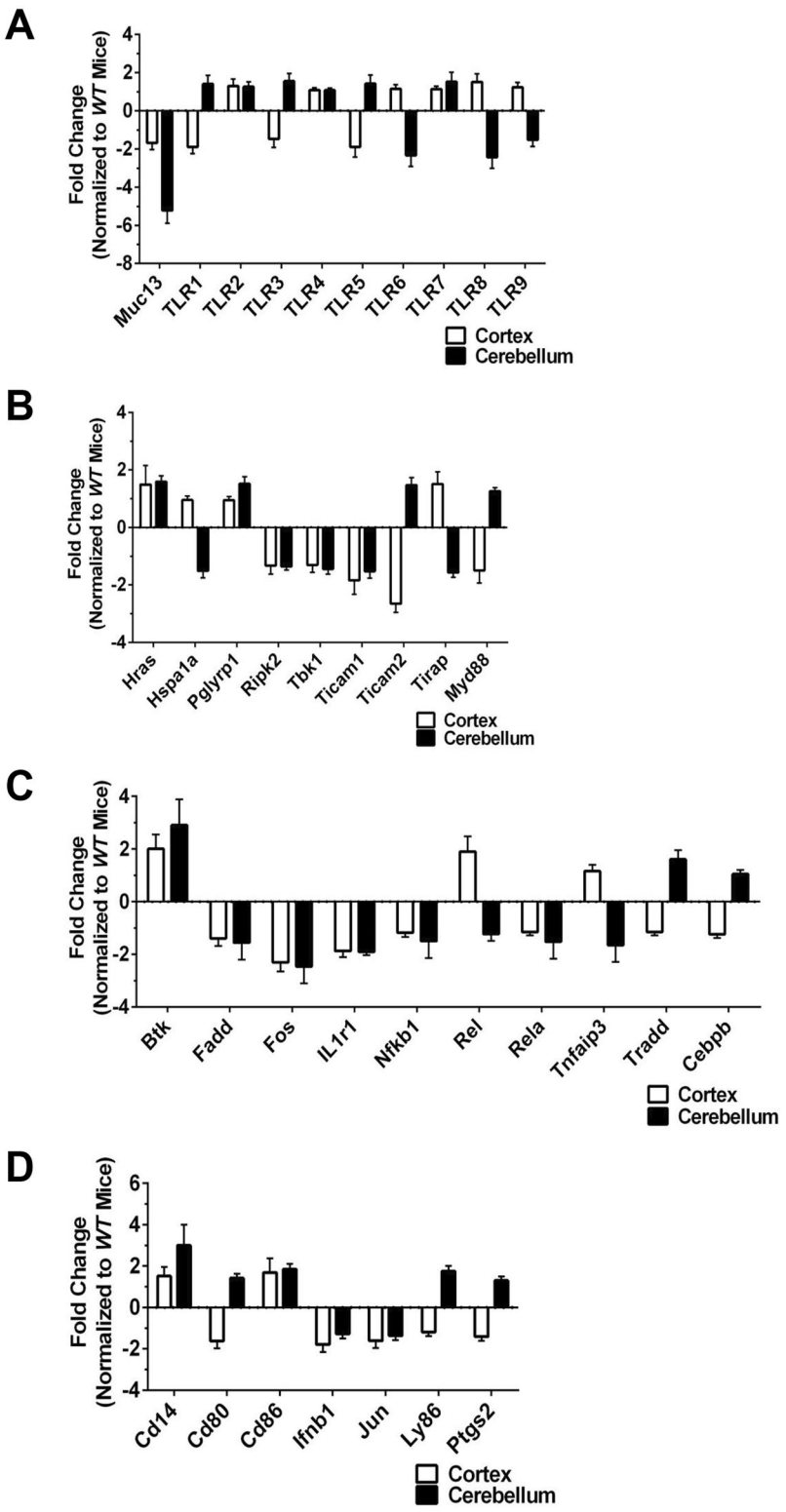

Fig. 5 Relative expression levels of toll-like receptors (TLR) (**A**), TLR interacting proteins & adaptors (**B**) signaling downstream of TLRs (**C**) and pathogen-specific response genes mRNA expression in 9-month-old *Neu4-/-* mice brain cortex and cerebellum, normalized to *WT* mice (n = 2)

For the expression analysis of apoptosis-related genes, mouse sialidase genes (Neu1, Neu2 and Neu3) and α-2,3 sialyltransferase gene, RNA isolation from cortex and cerebellum or total brain homogenetes of *WT* and *Neu4-/-* mice (n = 3) were performed using Trizol Reagent according to the manufacturer's instructions. Fifty ng/µl

of cDNA was synthesized by the High-Capacity cDNA Reverse Transcription kit (Applied Biosystems) according to manufacturer's instructions. The Real-Time PCR conditions were optimized using the LightCycler 96 machine (Roche, Swiss) with 75 ng of cDNA in the 20 µl of reaction mix containing 0.4 µM of primer pair and 1X LightCycler 480 SYBR Green I Master Mix (Roche, Swiss). The conditions of PCR were denoted as in the following: 1 cycle of 10 min at 95 °C; 45 cycles of 20 s at 95 °C, 15 s at 61 °C, and 22 s at 72 °C. The values were read after each cycle. In the end, the amplification melting analysis was performed under the following conditions: 30 s at 95 °C, 10 s at 60 °C, then continuous reading while the temperature increased to 99 °C, in order to detect the primer dimers if there were any. The primers used to amplify the mRNA are listed in Table 1.

Histopathology, immunohistochemistry (IHC) and tunel analysis

Mice were deeply anesthetized (Ketamine/Ketasol mixture; 200/10 mg/kg) followed by intracardiac perfusion into the left ventricle, firstly with 0.9% saline solution and then 4% paraformaldehyde (PFA) in phosphate buffer saline (PBS). Samples were incubated in the 4% PFA overnight at 4ºC and after that they were treated sequentially with 10% and 20% sucrose solutions for 2 h followed by 30% sucrose solutions overnight. Samples were embedded into the Tissue-Tek OCT compound (Sakura Finetechnical, Japan) and were stored at -80 ºC.

Fixed brain samples of *WT* and *Neu4-/-* mice were sectioned in the coronal plane at a 10 µm thickness using a Leica cryostat. Sectioned samples were placed on coated Histo-Bond® microscope slides (Marienfeld, Germany) at -20 °C. Ten µm sectioned samples were stained with Gill's hematoxylin (Merck, Germany) for 3 min and followed by counterstain 0.5% eosin Y solution (Merck, Germany) for 1 min. For periodic acid-Schiff reagent (PAS) staining, samples were stained with 0.5% Periodic acid for 5 min and Schiff reagent for 15 min according to the manufacturer's instructions (Merck, Germany). Counterstaining of the samples were performed with Gill's hematoxylin (Merck, Germany). All histological sections were mounted with Cytoseal 60.

Coronal brain slices (10 µm thickness) from the mice at the indicated ages were treated with ice-cold acetone, and then, blocked using blocking buffer (4% BSA, 10% goat serum, 0.3% Triton X-100 and 0.3 M glycine in PBS), for 1 h at room temperature in a humidified chamber. anti-LAMP1 (1:500; Abcam, USA), anti-Moma2 (1:50; Abcam, USA), anti-CNPase (1:50; Cell Signaling, Netherlands), anti-GFAP (1:200; Cell Signaling, Netherlands), anti-CD45 (1:100; Santa Cruz Biotechnology, USA) and anti-Iba1 (1:200; Cell Signaling, Netherlands) were diluted in blocking buffer and applied

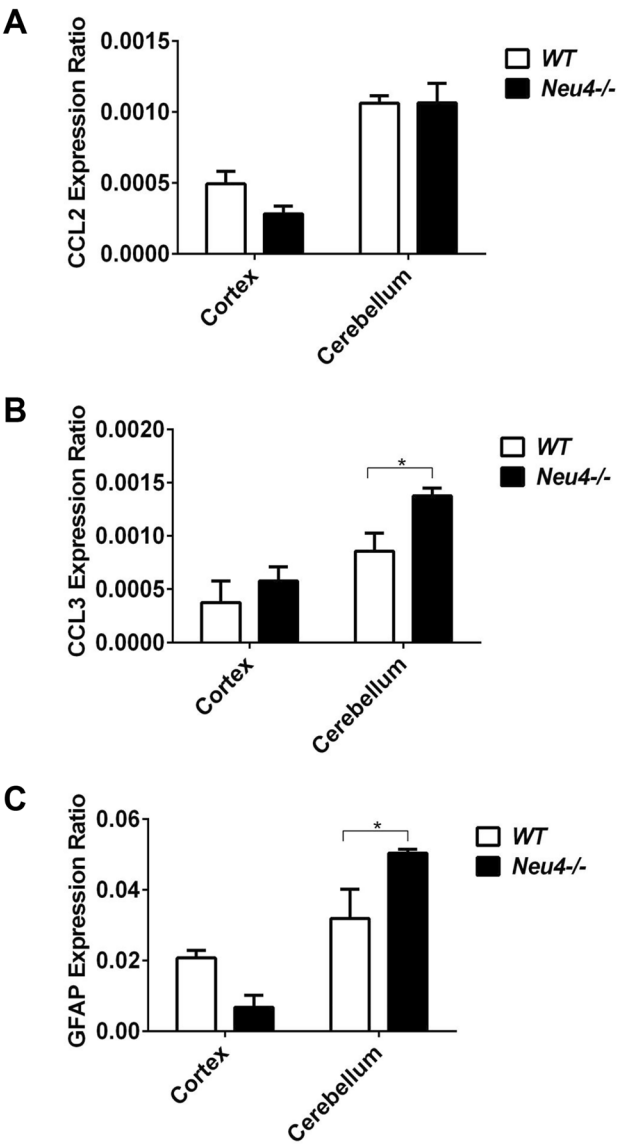

Fig. 6 Relative expression levels of CCL2 (**A**), CCL3 (**B**) and GFAP (glial fibrillary associated protein) (**C**) genes in 9-month-old *WT* and *Neu4-/-* mice cortex and cerebellum. The data are represented as the mean ± SEM. Two-way ANOVA was used for statistical analysis (*$p < 0.05$) (n = 2)

overnight at 4 °C. The Alexa Fluor conjugated secondary antibodies was used to visualize primary antibodies; goat anti-rabbit Alexa Fluor 488 (Abcam, USA), goat anti-rabbit Alexa Fluor 568 (Abcam, USA). The slides were mounted with Fluoroshield mounting medium with DAPI (Abcam, USA) and images were obtained using a light microscope (Bx53, Olympus Corporation, Germany) equipped with a manually controlled specimen holder; a color camera; a fluorescent light source; and image analysis software (cellSens Entry, Olympus Corporation, Germany). TUNEL (terminal deoxynucleotidyl

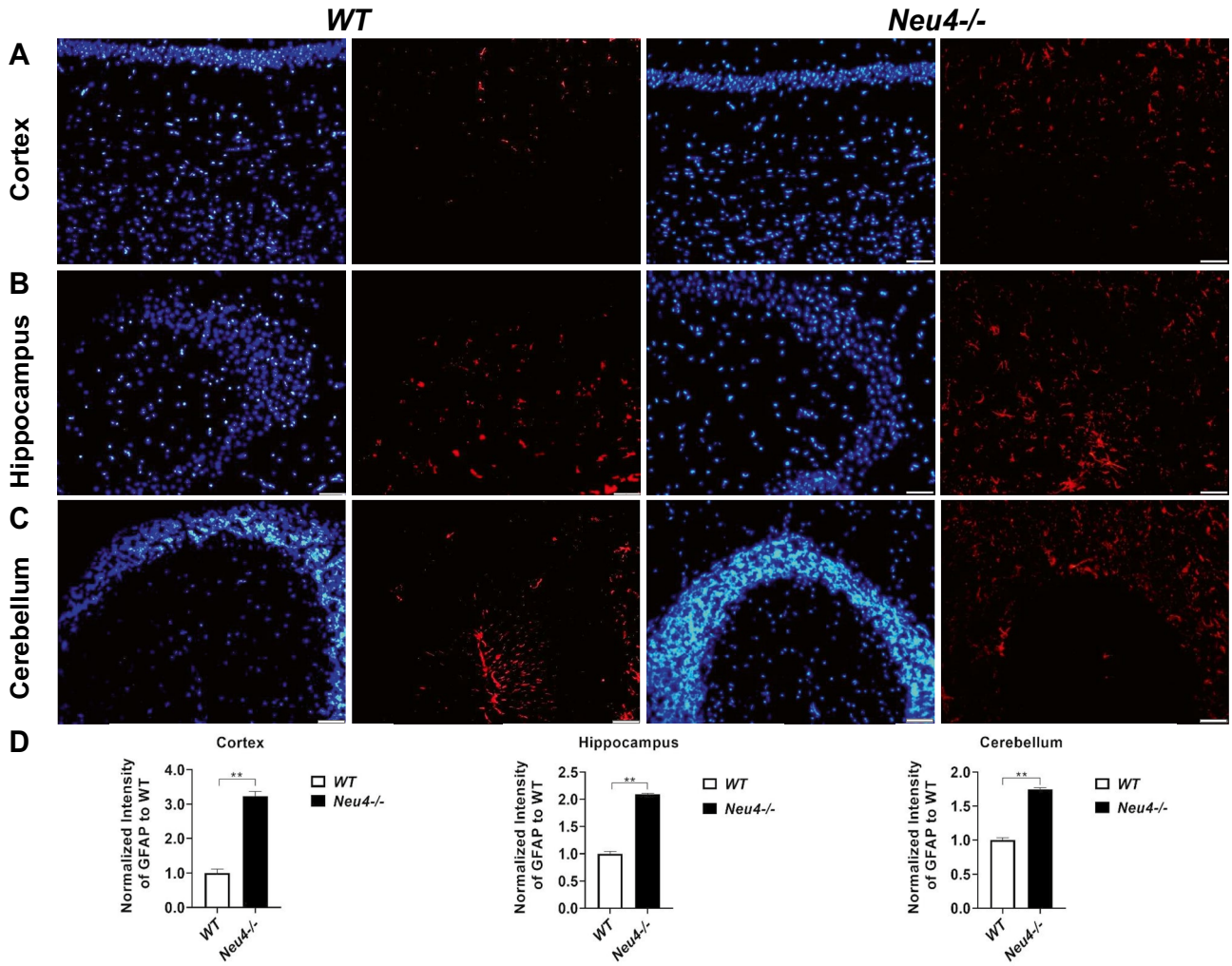

Fig. 7 Immunofluorescent staining of the astrocyte marker in *Neu4-/-* mouse brain sections. Brain sections of cortex (**A**), hippocampus (**B**) and cerebellum (**C**) from 9-month-old *WT* and *Neu4-/-* mice were stained with anti-GFAP(red) and DAPI(blue) Scale bar = 50 µm. (**D**) Quantitative analysis of the GFAP fluorescence intensity for each mice brain sections. The data are represented as the mean ± SEM. Unpaired t-test was used for statistical analysis (**p < 0.01)

transferase dUTP nick end labeling) staining was applied using ApopTag Fluorescein in Situ Apoptosis Detection Kit (Merck, Germany) following manufacturer's instructions. Fixation of brain sections were done with paraformaldehyde and ethanol:acetic acid solution (2:1). Fixed slides were incubated into the terminal deoxynucleotidyl transferase and then slides were incubated into anti-digoxigenin conjugate. Propidium iodide solution (0.5 µg/mL) was used as a nuclear counterstain. Fluorescent imaging of the TUNEL Assay was detected with a fluorescent microscope. Any positive green signals that indicate apoptosis were measured in the cortex, hippocampus and cerebellum respectively. The concentration of apoptotic signals was analyzed with ImageJ software (Java-based image processing program).

Behavioral analysis

Rotarod test: The balance and coordination ability were tested by rotarod test not only in 9 months old but also in 3, 6, and 12 months old *Neu4-/-* mice and age-matched *WT* mice. Firstly, mice were trained on the rotarod unit at 4 rpm. After the training period, mice were tested on the accelerated rotarod unit from 4 to 40 rpm over 5 min. Three trials were carried out for each animal and the duration times of mice were recorded on the accelerated unit. Prior to testing each animal, the rotarod units were cleaned by using 70% EtOH.

Passive avoidance test: Passive avoidance test was used to measure memory of the rodents in which 6, 9 and, 12-month-old *Neu4-/-* mice memory compared with the

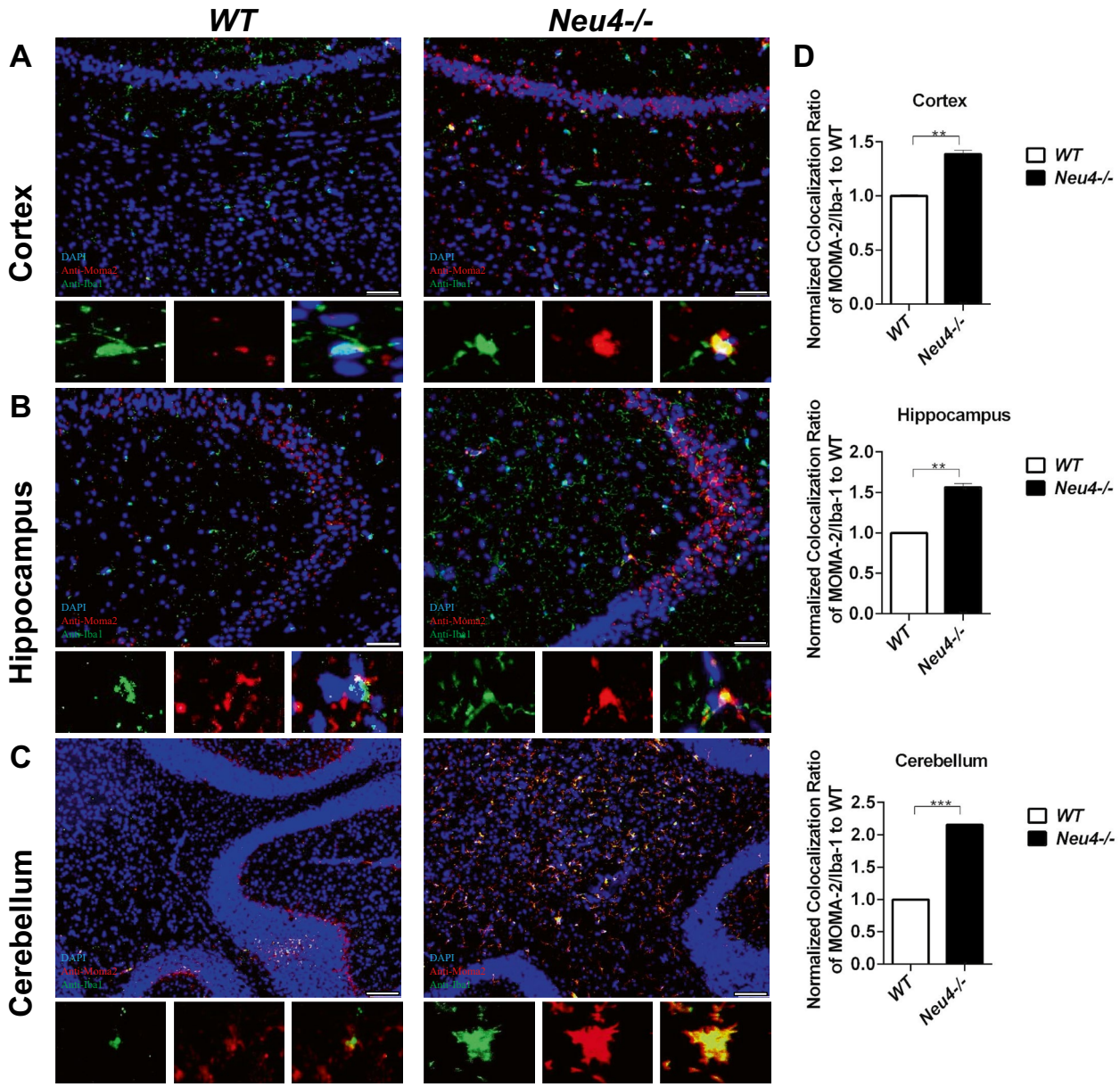

Fig. 8 Immunofluorescent detection of the microglial activation in *Neu4-/-* mouse brain sections. Brain sections of cortex (**A**), hippocampus (**B**) and cerebellum (**C**) from 9-month-old *WT* and *Neu4-/-* mice were stained with anti-Moma-2(red), anti-Iba-1(green) and DAPI(blue) Scale bar = 50 μm for cortex and hippocampus; 100 μm for cerebellum. (**D**) Quantitative analysis of the Moma-2 fluorescence intensity for each mouse brain sections. (**p < 0.01)

same age groups of *WT* mice. The apparatus is divided into two compartments; a lit compartment and a dark compartment, separated by a vertical sliding door between the two. Animals explore both compartments on the first day. Each mouse was put into the bright compartment, and then the central door opens after 30 s which allows the mouse to migrate into the dark compartment, an environment which the animal generally prefers due to light irritation. The following day, upon entry into the dark compartment, the door is closed, and the mouse is exposed a mild electric shock (0.2 mA for 2 s). On the final day, animals are given the same choice to enter the dark compartment (300 s maximum time). Latency to cross through the door between compartments was scored with ShutAvoid v1.8 (Harvard Apparatus, USA).

Open field test: The open field test is a sensorimotor test that was conducted in a box with a 40 × 40 cm surface area and transparent walls. Anxiety behaviors of 6, 9 and 12-month-old *Neu4-/-* mice compared with the same age groups of *WT* mice were studied. A digital camera was

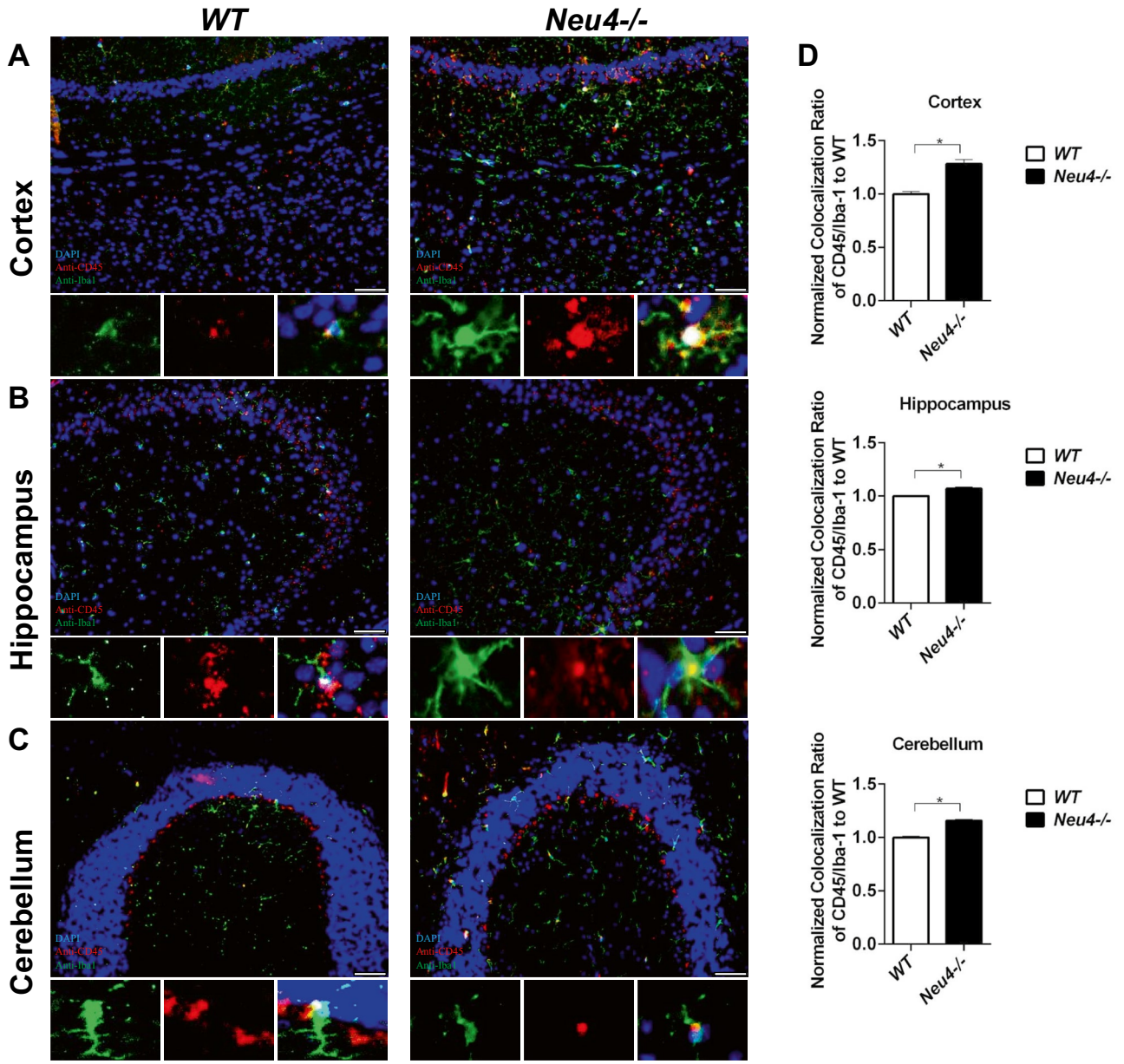

Fig. 9 Representative immunofluorescent staining of CD45 in *Neu4-/-* mouse brain sections. Brain sections of cortex (**A**), hippocampus (**B**) and cerebellum (**C**) from 9-month-old *WT* and *Neu4-/-* mice were stained with anti-CD45(red), anti-Iba-1(green) and DAPI(blue) Scale bar = 50 μm. (**D**) Quantitative analysis of the CD45 fluorescence intensity for each mice brain sections. The data are represented as the mean ± SEM. Unpaired t-test was used for statistical analysis (**p < 0.01)

placed directly on top of the box. Mice were put into a corner of the box to roam in the area undisturbed for 5 min. Behavioral differences were analyzed using the Panlab SMART Video Tracking System v0.3 (Harvard Apparatus, USA).

Hot plate test: Nociceptive heat sensitivity was assessed by hot plate test (IITC Life Science) in 3, 6, 9, and 12-month-old *Neu4-/-* mice compared to *WT*. The plate (10 × 20 × 30 cm) was heated to 55℃ and then each mouse was placed on it. Latency time of paw licking, shaking or hind paw licking and jumping were recorded for each mouse. A duration of 200 s was determined as the cut-off time. In addition, the hot plate test was applied as only one trial for each mouse because, they can learn the experiment in the short of a duration. Statistical analyses were determined by a two-way ANOVA with GraphPad Prism software. Significance was defined as $p < 0.05$. Each result is presented as ± SEM (Standard Error Mean).

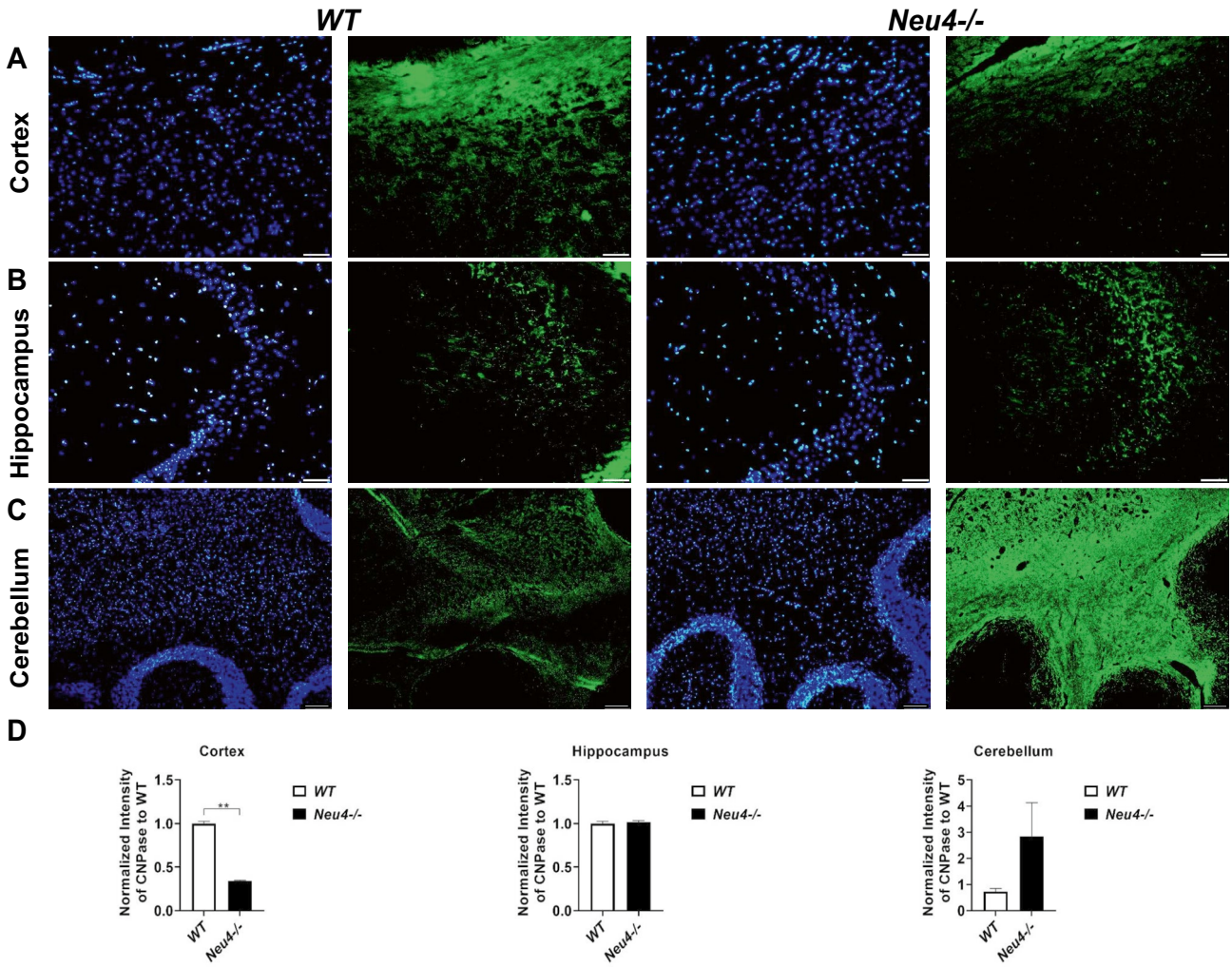

Fig. 10 Immunofluorescent staining of the oligodendrocytes in *Neu4-/-* mouse brain sections. Brain sections of cortex (**A**), hippocampus (**B**) and cerebellum (**C**) from 9-month-old *WT* and *Neu4-/-* mice were stained with anti-CNPase(green) and DAPI(blue) Scale bar = 50 µm. (**D**) Quantitative analysis of the CNPase fluorescence intensity for each mice brain sections. The data are represented as the mean ± SEM. Unpaired t-test was used for statistical analysis (**p < 0.01)

Results

Increased GD1a/GM1 ratio in brain

Significantly increased levels of GD1a, GT1b and decreased levels of GM1 gangliosides in cortex were displayed using thin layer chromatography method (Fig. 1A) similar to previously published data [23]. Ganglioside profiling revealed that the GD1a/GM1 ratio in 9-month-old *Neu4-/-* mice was increased 2.6-fold compared to *WT* mice (Fig. 1B). Although GT1b level is slightly elevated in *Neu4-/-* mice compared to *WT,* we detected no significant change in the level of LacCer and GD1b (Fig. 1C). We observed the similar ganglioside profile in cortex of 6-month-old *Neu4-/-* mice, suggesting progressive changes in ganglioside sialome. Although the level of GD1a in the cortex was not changed in younger mice, we demonstrated changes in the levels of GM1, GT1b and GD1b (Fig. S1). We also showed that the expression levels of ST3GAL3 significantly increased in the cortex of 12-month-old *Neu4-/-* mouse compared with WT, consistent with altered ganglioside profile in older age (Fig. 1D). Surprisingly, no significant changes in the mRNA level of ST3GAL3 were detected in the cerebellum of *Neu4-/-* mice (Fig. 1E).

Increased lamp1 + cells in cerebellum

Immunofluorescence staining for Lamp1 (lysosome-associated membrane protein 1) in 9-month-old *Neu4-/-* mice indicated

elevations of Lamp1 expression in the cerebellum, hippocampus and cortex. We showed that the number of Lamp1 + cells significantly increased only in the cerebellar region of *Neu4-/-* mice compared to WT (Figs. 2C, 2D). Both cortex and hippocampus appeared affected but no obvious quantitative differences were observed (Figs. 2A, B, D).

Elevated level of apoptotic signals in cortex and cerebellum

In order to determine whether elevated GD1a/GM1 ratio is linked to apoptosis in *Neu4-/-* brains, we performed immunohistochemical analysis with the TUNEL assay. We detected a significant elevation in apoptotic cell death (1.5-fold) in the hippocampal region of *Neu4-/-* mice compared to *WT*. There is a slightly increased number of Tunnel positive cells that were shown in cerebellum but not in cortex of 9-month-old *Neu4-/-* mice (Figs. 3A, C). The expression level of apoptosis-related genes was also determined in the cortex region of *Neu4-/-* mice by RT-PCR. Bcl-2 and Bcl-xL expression was evident only in cortex region (Figs. S2A, B). Interestingly, we found elevated level of pro-apoptotic Bax gene expression the same region (Fig. S2C). Although the ER-stress associated ATF6 gene expression was moderately high in cerebellum, Calnexin which is another ER-stress related gene was not increased either in the cortex or cerebellum of *Neu4-/-* mice (Figs. S2D, E). The level of oxidative stress related SOD2 in cortex and cerebellum showed no significant difference between *Neu4-/-* and *WT* control mice (Fig. S2F).

Elevation of inflammatory chemokines and cytokines in cortex and cerebellum

Expression levels of pro-inflammatory chemokines in 9 months old *Neu4-/-* mice displayed Ccl11, 5.1 and 3.6 fold; Ccl3, 1.7 and 3.4 fold; Ccl4, 0.8 and 5.8 fold; Ccl5 1.6 and 1.9 fold; Cxcl10, 1.4 and 1.3 fold; Cxcl11, 1.7 and 5.4 fold; Cxcl3, 7.1 and 6.5 fold; Cxcl5, 4.7 and 1.4 fold; Cxcl9, 2.8 and 14.8 fold increases in both cortex and cerebellum, respectively (Fig. 4A). Expression of pro-inflammatory cytokines elicited IL1rn 1.9 and 4.8 fold; IL21, 2.4 and 3.5 fold; IL27, 3.3 and 13.7 fold; IL3, 1.9 and 3.4 fold; IL9, 1.9 and 8.8 fold; Tnf, 1.1 and 9.9 fold; Ifna2, 1.9 and 15 fold; Ifng, 1.2 and 8.7 fold increases in cortex and cerebellum of 9 months old *Neu4-/-* mice, respectively (Fig. 4B).

Despite augmentation in pro-inflammatory chemokines and cytokines, an overall increase was exhibited in the expression levels of anti-inflammatory chemokines and cytokines (Fig. 4C). With respect to anti-inflammatory chemokines Ccl19 increased 1.7 and 2.4-fold in cortex and cerebellum of *Neu4-/-* mice, respectively. The anti-inflammatory cytokines IL10 increased 5.4 and 9.5-fold; IL24, 4.3 and 3.4-fold in cortex and cerebellum, respectively but,

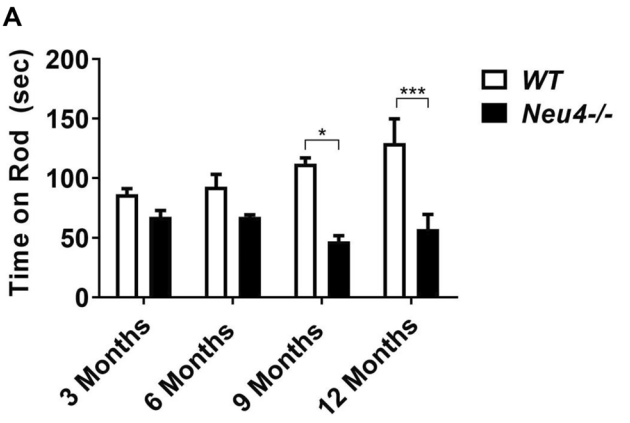

Fig. 11 Behavioral tests in *Neu4-/-* mouse model. Rotarod tests of 3, 6, 9, 12-month-old *Neu4-/-* mice compared to *WT*. 3-month-old *WT* (n = 12), *Neu4-/-* (n = 7); 6-month-old *WT* (n = 12), *Neu4-/-* (n = 7); 9-month-old *WT* (n = 16), *Neu4-/-* (n = 21); 12-month-old *WT* (n = 13), *Neu4-/-* (n = 12). The data are represented as the mean ± SEM, Multiple t test was used for statistical analysis (**p < 0.01, *** p < 0.005)

IL2 (6.9 fold), IL13 (11-fold) and IL22 (10.1-fold) only increased in cerebellum (Fig. 4C). Moreover, IL11, IL 23a and Tgfb2 anti-inflammatory cytokine gene expression levels decreased in only cortex with 1.9, 1.7 and 1.5-fold changes, respectively.

Altered expression level of TLR signaling pathway related genes

Deficient sialidase Neu4 in mice elicited differential expression of TLR-associated signaling pathway genes compared to *WT*. Muc13 decreased 1.5 and 4.8 fold in both cortex and cerebellum of *Neu4-/-* mice respectively as well as decreased levels of TLR1 (1.7 fold), TLR3 (1.9 fold) and TLR5 (1.6 fold) in only cortex; TLR6 (twofold), TLR8 (twofold) and TLR9 (1.5 fold) in only cerebellum of *Neu4-/-* mice (Fig. 5A). In addition, TLR2 (1.3 and 1.3 fold), TLR4 (1.1 and 1.1 fold) and TLR7 (1.1 and 1.5 fold) RNA expressions enhanced in both cortex and cerebellum. The TLR interacting proteins and adaptors gene expression levels of Ticam1 (1.6-fold) and Ticam2 (2.5-fold) significantly decreases in the cortex region (Fig. 5B). Decreased expression was also observed in the analyzed downstream molecules of TLRs, except Rel 1.6-fold in the cortex region of *Neu4-/-* mice. Major decreases especially in Fos (1.9 and 2.2-fold) and IL1r1 (1.4 and 1.9-fold) were found in *Neu4-/-* mice compared to *WT* (Fig. 5C). Although Cd14, Cd86 and Ly86 were increased up to twofold in both the cortex and cerebellum, Ifn1b and Jun decreased 1.9 and 1.7-fold in cortex and 1.5-fold in cerebellum for *Neu4-/-* mice compared to *WT* (Fig. 5D).

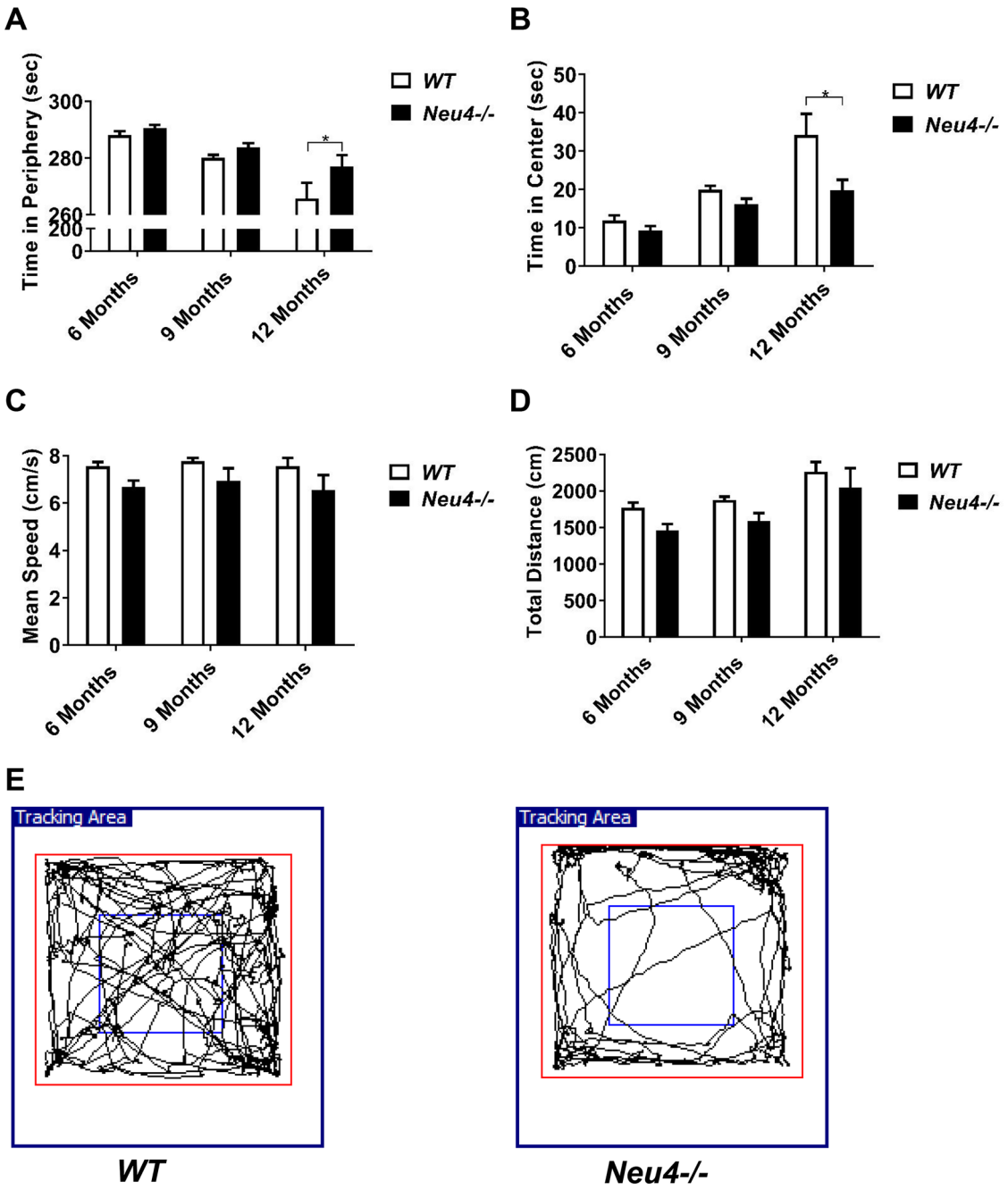

Fig. 12 Anxiety and locomotor activity were tested for 6, 9 and 12-month-old *WT* and *Neu4-/-* mice with open field analysis. Time spent in the periphery (**A**), the center (**B**), total distance (**C**) and mean speed (**D**) in the open field area were analyzed. 6-month-old *WT* (n = 6), *Neu4-/-* (n = 6); 9-month-old *WT* (n = 5), *Neu4-/-* (n = 5); 12-month-old *WT* (n = 13), *Neu4-/-* (n = 11) mice. Schematic drawings of the zones and representative traces of 12-month-old (**E**) mice movements during the test. The data are represented as the mean ± SEM. Multiple t test was used for statistical analysis. (*$p < 0.05$)

Altered expression levels of glial markers

Microglial markers Ccl2, Ccl3 and GFAP displayed various expression patterns in the different brain regions of *Neu4-/-* mice. Ccl3 and GFAP exhibited significant changes only in the cerebellar region of 9-month–old *Neu4-/-* mice brain compared to *WT* (Figs. 6B, 6C) but Ccl2 did not show significant expression differences in both the cortex and cerebellum (Figs. 6A). To evaluate the increasing mRNA expression of the GFAP marker in the cerebellar region, GFAP staining was applied to the brain of *Neu4-/-* mice. Interestingly, GFAP staining displayed significantly higher

number of GFAP + cells not only in cerebellum but also in hippocampus and cortex brain region of *Neu4-/-* mice compared to *WT* (Figs. 7A, D).

Elevation of PBMC infiltration and macrophage activity

Peripheral blood mononuclear cellular (PBMC) infiltration is one of the signs of neuroinflammation in the brain of mouse models with lysosomal storage disease. The elevation of PBMC infiltration was reported in the Sandhoff mouse model [42]. We showed PBMC infiltration using CD45 staining. *Neu4-/-* and *WT* brain sections were stained with anti-CD45/anti-Iba1 and anti-Moma2/anti-Iba1. The colocalized microglial marker of Iba1 and CD45-positive cells increased both in hippocampus and cerebellum (Figs. 8B, C, D) compared to *WT* but interestingly colocalized CD45-positive cells remained low in the *Neu4-/-* cortex compared to *WT* (Figs. 8A, D). Similarly, we demonstrated significantly higher levels of macrophage activation in the cerebellum of Neu*4-/-* mice (Fig. 9C) but it was decreased in the cortex and hippocampus (Figs. 9A, B). Oligodendrocytes are the myelinating glia cells found in the CNS. The myelination process is carried by these cells [43]. Moreover, low oligodendrocyte number correlates with neuroinflammation [44]. Therefore, CNPase staining was applied to demonstrate whether demyelination process is associated with neuroinflammation. CNPase staining showed significantly low numbers of oligodendrocytes in the cortex (Fig. 10A) compared to *WT* but, there was no significant differences in the hippocampus and cerebellum (Figs. 10B, C, D).

H&E staining showed the absence of vacuolization in neurons in the cortex and hippocampus and a normal Purkinje cell layer in cerebellum of *Neu4-/-* and *WT* mice (Fig. S3). We also demonstrated non-significant PAS-positive granules between 9-month-old *Neu4-/- and WT* mice brain sections (Fig. S4).

Deficits in cerebellar motor coordination in *Neu4-/-* mice

The rotarod analysis of 3, 6, 9 and 12-month-old *Neu4-/-* mice exhibited impaired cerebellar motor activity compared with controls. The rotarod activity test is a behavioral method which measures motor activity and balance for murine models. The first trial was delineated as the habituation period for this test and then three additional three trials are performed compared with control. The four different age groups of *Neu4-/-* mice performed significant result compared with the same age groups of control mice (Fig. 11).

Increasing anxiety-related behavior in *Neu4-/-* mice.

The anxiety levels of the mice were measured with the 5-min open field test. Three different age groups (6, 9 and 12-month-old) of the *Neu4-/-* mice model were compared to the same age groups of *WT*. A slight difference was only detected between 12-month old *Neu4-/-* and *WT* mice but not in other age groups. The 12-month-old *Neu4-/-* mice (277,1 ± 4,44 s) spent more time in the periphery of the open field maze than the *WT* mice (265.8 ± 4,29 s) (Figs. 12A, B). Total distance and mean speed values exhibited non-significant differences into *Neu4-/-* mice compared to *WT* mice in each age group (Figs. 12C, D). The walking patterns of the 12-month-old *Neu4-/-* mice (Fig. 12E) as well as the time spent in the periphery and the center of the open field box indicated more anxiety-related behavior compared to the same age group of *WT* mice.

In an effort to address whether neuroinflammation in nociceptive pathways contribute to the generation of pain in *Neu4-/-* mice, we used sensorimotor task to determine acute thermal pain. *Neu4-/-* mice displayed no differential sensitivity to acute, thermal nociception as measured on the hot-plate assay (Fig. S5). The passive avoidance test was also used to indicate fear memory deficits. *Neu4-/-* showed no significant differences in retention comparison to WT mice (Fig. S6).

Discussion

A previously generated sialidase Neu4 deficient mouse was viable, fertile, and displayed no gross morphological abnormalities, but showed a marked vacuolization and lysosomal storage in lung and spleen cells. Their ganglioside pattern demonstrated an increased level of GD1a and GT1b gangliosides as well as a markedly decreased level of the GM1 ganglioside in the brain [23]. Presently, we showed a significantly increased GD1a/GM1 ratio in the *Neu4-/-* mouse brain, as 2.6-fold, compared to *WT* (Figs. 1A, B). In an effort to address whether sialidase Neu4 alone, not accompanied with sialidase Neu3 mediate inflammatory conditions, we examined neuroinflammation markers and behavioral phenotypes in sialidase Neu4 deficient mouse. Using molecular genetics and immunohistochemical techniques, we demonstrated that 9-month-old mice have increased neuroinflammation and apoptosis in cortex, hippocampus and cerebellum that correlated with relatively mild behavioral alterations.

Gangliosides, sialic acid containing glycosphingolipids are major components of neural membranes, being localized at membrane microdomains, lipid rafts, and contribute to crucial biological processes in brain physiology and pathology. In eukaryotic cells, gangliosides mainly function in signal transduction, cell adhesion, modulating growth factor/hormone receptors, antigen recognition, and protein trafficking [45]. A balance is found between the anabolism and catabolism of gangliosides. They are transported to the lysosomes of the cells by endocytosis, being degraded wit

a complex mechanism by the sequential release of carbohydrate and sialic acid residues, involving enzymes, activator proteins and negatively charged lipids [46]. While abnormalities in ganglioside degradation result in accumulation of undegrated gangliosides in lysosomes, removal or non-removal of a sialic acid residue from each ganglioside would affect different cellular pathways [47]. It has been reported that TLRs respond to ganglioside activation and trigger ganglioside-stimulated intracellular inflammatory signaling in the rat brain [30]. Consistent with this finding, our gene expression profiling revealed that a sialidase Neu4 deficiency causes not only elevated level of neuroinflammation markers in both the cortex and cerebellum but also significantly alters signaling pathway related to TLR genes which are involved in the initial phase as the sensors of different pathogens and tissue damage.

Cytokines are small secreted proteins that have a specific effect on the interactions and communications between cells. Moreover, chemokines are a superfamily of secreted small molecules involved in immune-regulatory and inflammatory processes [48, 49]. Increased levels of chemokines and their respective receptors have been found in numerous pathological conditions. Studies showed changes in ganglioside composition as well as in the inflammatory cytokine/chemokine genes expression levels in several LSDs with central nervous system involvement [32]. In normal conditions, microglial cells stay in the inactive stage, but the accumulated macromolecules activate microglial cells causing an increased inflammatory response indicating that this process has a significant contribution to disease pathology [33]. Ccl2 (MCP1, Monocyte Chemotactic Protein 1) displays chemotactic activity for monocytes, lymphocytes and for neutrophils and Ccl4 (MIP1-β, Macrophage Inflammatory Protein 1-β) to activate T cells and macrophages [49]. Cxcl9, Cxcl10, and Cxcl11 are also key elements of inflammation mediated by T cells [50]. Up to 16.7-fold up-regulation in these chemokine genes and up to 17 fold up-regulation in cytokine genes such as IL1rn, IL27, IL9, Tnf, Ifna2 and Ifng in the cerebellum indicate that there was an inflammatory response in this brain region of *Neu4-/-* mice. The alteration in the expression levels of inflammatory cytokines and chemokines in the cortex was significant but not as high as the cerebellum. This increase that was seen in anti-inflammatory chemokine and cytokine gene expression levels may be due to a feedback mechanism designed to stop or regulate the inflammatory response in both the cortex and cerebellum of *Neu4-/-* mice.

Previously it was shown that gangliosides induce inflammation via TLR4 [30] and when Neu4 was induced with thymoquinone, there is activation of the NFκB signaling pathway via TLR4 [51]. Although the expression level of TLR4 did not change significantly in the cortex and cerebellum of *Neu4-/-* mice, we suggest that the altered expression ratio of Muc13, TLR1, 5, 8 and 9 might be responsible for the changing the expression level of NFκB, Jun and Fos signaling pathway molecules and increased expression of chemokines and cytokines in *Neu4-/-* mice.

Altered levels of GD1a and GM1 gangliosides have been shown to function in MAPK and NFκB signaling pathways via TLR4 [52] by inhibiting its translocation into lipid rafts [53]. Since the levels of both GD1a and GM1 gangliosides were altered in Neu4 deficient mice, inflammatory cascades were triggered and the expression ratio of other related genes were affected by this situation in a positive or negative manner that contributes to both inflammation and break down of different cellular pathways. Although there was no pathogen induction in these mice, we observed up and down-regulations in pathogen specific response gene expression ratios which suggests that that there are novel signaling cascades that might also contribute to neuroinflammation in the brain. Interestingly, we showed Btk has the most distinct elevated level of expression in both the cortex and cerebellum (1.9 and 2.6-fold respectively) of *Neu4-/-* mice. Btk is a nonreceptor tyrosine kinase, interacting with a subdomain of TLR, involved in the activation of transcription factors that regulate B cell development, antibody production, and immune responses [54]. Deletion of Btk gene in *Btk-/-* mice resulted in a reduced level of macrophage polarization and recruitment in response to lipopolysaccharide induction [55] which demonstrate that Btk is the responsible molecule in macrophage mediated inflammation. Altered ganglioside levels in cells (increased GD1a/GM1 ratio and/or GT1b) might be responsible for the higher expression level of Btk in *Neu4-/-* mice brain which results in altered signaling and increased inflammatory response.

Nitric oxide (NO) is a signaling molecule that plays a key role in regulation of acute and chronic inflammation, neurotransmission, and host-defense mechanism [56]. It has dual role as an anti-inflammatory and as a pro-inflammatory mediator in normal and abnormal situations respectively. NO is involved in immune responses by cytokine-activated macrophages, which release high levels of NO. In addition, NO is a potent neurotransmitter at the neuron synapses and contributes to the regulation of apoptosis. Previously, with *in vitro* analyses we determined primary bone marrow macrophage cells derived *Neu4-/-* mice exhibited a significant increase in endotoxin LPS-induced NO production compared to the *WT* control [32]. Here, we provide *in vivo* evidence that sialidase Neu4 is involved the release of NO initiated by inflammatory cytokines and macrophage activation which is most likely due to a desialylation deficit in neural membrane gangliosides in the mice brain.

Minami et al. investigated the effect of sialidase Neu4 knockdown on hippocampus-dependent spatial memory by using the Morris water maize. They reported that DANA (a sialidase inhibitor) or siRNA targeting Neu4 that were injected into the rat cerebral ventricle causes significantly

impaired hippocampal memory but not motility [57]. Similarly, we assessed spatial learning and memory in a water maze task. Interestingly, *Neu4-/-* mice showed no significant impairment in spatial learning (data not shown). In contrast, *Neu4-/-* mice displayed slight reduced activity in exploratory pattern in open field (corners vs center). Motor coordination on the rotarod also appeared affected in *Neu4-/-* mice between 9 and 12 months of age. These results are consistent with increases in LAMP1 expression and neuroinflammation markers in cerebellar areas. Although no major differences in the degrees of pathology were observed, increased level of Tunel positive cells and low number of oligodendrocytes in *Neu4-/-* mice remains an open question and further experiments are required to clarify the role of desialylation function of sialidase Neu4 in altered ganglioside pattern associated with neuroinflammation and neurodegeneration.

Previously, it has been reported that the levels of Neu3 and Neu4 mRNA were significantly increased in the brain tissues of *Neu4-/-* and *Neu3-/-* mice, respectively which suggested the existence of mechanisms for compensatory regulation between the Neu3 and Neu4 genes [40]. Regarding comparative expression levels of other sialidases in total brain homogenates of 9-month-old *Neu4-/-* mice, our data indicate that three forms (Neu1, Neu2 and Neu3) display same patterns of expression suggesting that they do not compensate lack of sialidase Neu4 (Fig. S7) but further studies are required to clarify whether sialidase Neu4 deficiency effect the expression level of other sialidases in specific region of mouse brain.

In summary, our results suggest that the increase in the level of GT1b and GD1a/GM1 ganglioside ratio in the cerebellum and cortex in mice due to lack of sialidase Neu4 triggers a signaling cascade that either activates or represses neuroinflammation via direct alterations in the level of chemokine and cytokine gene expression levels or indirectly via the TLR related signaling pathways. Numerious data has provided a growing body of evidence for great importance of sialidases in cellular functions and significance of physiological and pathological desialylation process. Although the definite target molecules for sialidase Neu4 have yet to be identified, our data indicate that changes in gangliosides composition in *Neu4-/-* mice brain leads to the release of pro- and anti-inflammatory chemokines and cytokines that contribute to a complex inflammatory response including astrogliosis and microgliosis. We suggest that modulation of sialidase Neu4 genetic expression by Crispr/Cas9 system might be effective for improving neurological conditions where neuroinflammation is involved.

Supplementary information The online version contains supplementary material available at https://doi.org/10.1007/s10719-021-10017-9.

Acknowledgements This study was supported by the TUBİTAK 113T025 Grant to Prof. Dr. Volkan Seyrantepe. Zehra Kevser Timur is grateful to TUBITAK-BIDEB for scholarship support. Orhan Kerim İnci received a scholarship from the YOK 100/2000 program. We also thank Prof Dr. Michelle Adams from Bilkent University, Department of Psychology, Ankara, Turkey, for helpful advice and critical reading and editing of manuscript.

Compliance with ethical standards

Conflict of interest The authors declare that they have no conflicts of interest.

Ethics approval This article does not contain any studies with human participants or animals performed by any of the authors.

References

1. Miyagi, T., Yamaguchi, K.: Mammalian sialidases: physiological and pathological roles in cellular functions. Glycobiology **22**(7), 880–896 (2012). https://doi.org/10.1093/glycob/cws057
2. D'Azzo, A., Hoogeveen, A., Reuser, A.J., Robinson, D., Galjaard, H.: Molecular defect in combined beta-galactosidase and neuraminidase deficiency in man. Proc. Natl. Acad. Sci. U.S.A. **79**(15), 4535–4539 (1982). https://doi.org/10.1073/pnas.79.15.4535
3. Galjart, N.J., Gillemans, N., Harris, A., van der Horst, G.T., Verheijen, F.W., Galjaard, H., d'Azzo, A.: Expression of cDNA encoding the human "protective protein" associated with lysosomal beta-galactosidase and neuraminidase: homology to yeast proteases. Cell **54**(6), 755–764 (1988). https://doi.org/10.1016/s0092-8674(88)90999-3
4. Miyagi, T., Takahashi, K., Yamamoto, K., Shiozaki, K., Yamaguchi, K.: Biological and Pathological Roles of Ganglioside Sialidases. Prog In Mole Bio And Trans Sci **156**, 121–150 (2018). https://doi.org/10.1016/bs.pmbts.2017.12.005
5. Akyildiz Demir, S., Seyrantepe, V.: Identification of cytoplasmic sialidase NEU2-associated proteins by LC-MS/MS. Turkish J Biochem **44**(4), 462–472 (2019). https://doi.org/10.1515/tjb-2018-0089
6. Sato, K., Miyagi, T.: Genomic organization and the 5'-upstream sequence of the rat cytosolic sialidase gene. Glycobiology **5**(5), 511–516 (1995). https://doi.org/10.1093/glycob/5.5.511
7. Tokuyama, S., Moriya, S., Taniguchi, S., Yasui, A., Miyazaki, J., Orikasa, S., Miyagi, T.: Suppression of pulmonary metastasis in murine B16 melanoma cells by transfection of a sialidase cDNA. Int. J. Cancer **73**(3), 410–415 (1997). https://doi.org/10.1002/(sici)1097-0215(19971104)73:3%3c410::aid-ijc16%3e3.0.co;2-g
8. Hasegawa, T., Yamaguchi, K., Wada, T., Takeda, A., Itoyama, Y., Miyagi, T.: Molecular cloning of mouse ganglioside sialidase and its increased expression in Neuro2a cell differentiation. J. Biol. Chem. **275**(11), 8007–8015 (2000). https://doi.org/10.1074/jbc.275.11.8007
9. Valaperta, R., Chigorno, V., Basso, L., Prinetti, A., Bresciani, R., Preti, A., Miyagi, T., Sonnino, S.: Plasma membrane production of ceramide from ganglioside GM3 in human fibroblasts. FASEB journal : official publication of the Federation of American Societies for Experimental Biology **20**(8), 1227–1229 (2006). https://doi.org/10.1096/fj.05-5077fje
10. Hahn, C.N., del Pilar Martin M., Schröder, M., Vanier, M.T., Hara, Y., Suzuki K., Suzuki K., d'Azzo, A.: Generalized CNS disease and massive GM1-ganglioside accumulation in mice defective in lysosomal acid beta-galactosidase. Hum Mol Genet Feb **6**(2), 205–11 (1997). https://doi.org/10.1093/hmg/6.2.205
11. Yamaguchi, K., Hata, K., Koseki, K., Shiozaki, K., Akita, H., Wada, T., Moriya, S., Miyagi, T.: Evidence for mitochondrial

localization of a novel human sialidase (NEU4). Biochem. J. **390**(Pt 1), 85–93 (2005). https://doi.org/10.1042/BJ20050017
12. Bigi, A., Morosi, L., Pozzi, C., Forcella, M., Tettamanti, G., Venerando, B., Monti, E., Fusi, P.: Human sialidase NEU4 long and short are extrinsic proteins bound to outer mitochondrial membrane and the endoplasmic reticulum, respectively. Glycobiology **20**(2), 148–157 (2010). https://doi.org/10.1093/glycob/cwp156
13. Shiozaki, K., Koseki, K., Yamaguchi, K., Shiozaki, M., Narimatsu, H., Miyagi, T.: Developmental change of sialidase neu4 expression in murine brain and its involvement in the regulation of neuronal cell differentiation. J. Biol. Chem. **284**(32), 21157–21164 (2009). https://doi.org/10.1074/jbc.M109.012708
14. Monti, E., Bassi, M.T., Bresciani, R., Civini, S., Croci, G.L., Papini, N., Riboni, M., Zanchetti, G., Ballabio, A., Preti, A., Tettamanti, G., Venerando, B., Borsani, G.: Molecular cloning and characterization of NEU4, the fourth member of the human sialidase gene family. Genomics **83**(3), 445–453 (2004). https://doi.org/10.1016/j.ygeno.2003.08.019
15. Monti, E., Bonten, E., D'Azzo, A., Bresciani, R., Venerando, B., Borsani, G., Schauer, R., Tettamanti, G.: Sialidases in vertebrates: a family of enzymes tailored for several cell functions. Adv In Carbohy Chem And Biochem **64**, 403–479 (2010). https://doi.org/10.1016/S0065-2318(10)64007-3
16. Comelli, E.M., Amado, M., Lustig, S.R., Paulson, J.C.: Identification and expression of Neu4, a novel murine sialidase. Gene **321**, 155–161 (2003). https://doi.org/10.1016/j.gene.2003.08.005
17. Pshezhetsky, A.V., Ashmarina, M.: Keeping it trim: roles of neuraminidases in CNS function. Glycoconj. J. **35**(4), 375–386 (2018). https://doi.org/10.1007/s10719-018-9837-4
18. Hildebrandt, H., Mühlenhoff, M., Weinhold, B., Gerardy-Schahn, R.: Dissecting polysialic acid and NCAM functions in brain development. J. Neurochem. **103**(Suppl 1), 56–64 (2007). https://doi.org/10.1111/j.1471-4159.2007.04716.x
19. Takahashi, K., Mitoma, J., Hosono, M., Shiozaki, K., Sato, C., Yamaguchi, K., Kitajima, K., Higashi, H., Nitta, K., Shima, H., Miyagi, T.: Sialidase NEU4 hydrolyzes polysialic acids of neural cell adhesion molecules and negatively regulates neurite formation by hippocampal neurons. J. Biol. Chem. **287**(18), 14816–14826 (2012). https://doi.org/10.1074/jbc.M111.324186
20. Yamanami, H., Shiozaki, K., Wada, T., Yamaguchi, K., Uemura, T., Kakugawa, Y., Hujiya, T., Miyagi, T.: Down-regulation of sialidase NEU4 may contribute to invasive properties of human colon cancers. Cancer Sci. **98**(3), 299–307 (2007). https://doi.org/10.1111/j.1349-7006.2007.00403.x
21. Silvestri, I., Testa, F., Zappasodi, R., Cairo, C.W., Zhang, Y., Lupo, B., Galli, R., Di Nicola, M., Venerando, B., Tringali, C.: Sialidase NEU4 is involved in glioblastoma stem cell survival. Cell Death Dis. **5**(8), e1381 (2014). https://doi.org/10.1038/cddis.2014.349
22. Hasegawa, T., Sugeno, N., Takeda, A., Matsuzaki-Kobayashi, M., Kikuchi, A., Furukawa, K., Miyagi, T., Itoyama, Y.: Role of Neu4L sialidase and its substrate ganglioside GD3 in neuronal apoptosis induced by catechol metabolites. FEBS Lett. **581**(3), 406–412 (2007). https://doi.org/10.1016/j.febslet.2006.12.046
23. Seyrantepe, V., Canuel, M., Carpentier, S., Landry, K., Durand, S., Liang, F., Zeng, J., Caqueret, A., Gravel, R.A., Marchesini, S., Zwingmann, C., Michaud, J., Morales, C.R., Levade, T., Pshezhetsky, A.V.: Mice deficient in Neu4 sialidase exhibit abnormal ganglioside catabolism and lysosomal storage. Hum. Mol. Genet. **17**(11), 1556–1568 (2008). https://doi.org/10.1093/hmg/ddn043
24. Seyrantepe, V., Lema, P., Caqueret, A., Dridi, L., Bel Hadj, S., Carpentier, S., Boucher, F., Levade, T., Carmant, L., Gravel, R.A., Hamel, E., Vachon, P., Di Cristo, G., Michaud, J.L., Morales, C.R., Pshezhetsky, A.V.: Mice doubly-deficient in lysosomal hexosaminidase A and neuraminidase 4 show epileptic crises and rapid neuronal loss. PLoS Genet. **6**(9), e1001118 (2010). https://doi.org/10.1371/journal.pgen.1001118
25. Sandhoff, R., Sandhoff, K.: Emerging concepts of ganglioside metabolism. FEBS Lett Dec **592**(23), 3835–3864 (2018)
26. Sturgill, E.R., Aoki, K., Lopez, P.H., Colacurcio, D., Vajn, K., Lorenzini, I., Majić, S., Yang, W.H., Heffer, M., Tiemeyer, M., Marth, J.D., Schnaar, R.L.: Biosynthesis of the major brain gangliosides GD1a and GT1b. Glycobiology **22**(10), 1289–1301 (2012). https://doi.org/10.1093/glycob/cws103
27. Regina Todeschini, A., Hakomori, S.I.: Functional role of glycosphingolipids and gangliosides in control of cell adhesion, motility, and growth, through glycosynaptic microdomains. Biochem. Biophys. Acta. **1780**(3), 421–433 (2008). https://doi.org/10.1016/j.bbagen.2007.10.008
28. Ryu, J.S., Ko, K., Ko, K., Kim, J.S., Kim, S.U., Chang, K.T., Choo, Y.K.: Roles of gangliosides in the differentiation of mouse pluripotent stem cells to neural stem cells and neural cells (Review). Mol. Med. Rep. **16**(2), 987–993 (2017). https://doi.org/10.3892/mmr.2017.6719
29. Furukawa, K., Ohmi, Y., Tajima, O., Ohkawa, Y., Kondo, Y., Shuting, J., Hashimoto, N., Furukawa, K.: Gangliosides in inflammation and neurodegeneration. Prog In Mole Bio And Trans Sci **156**, 265–287 (2018). https://doi.org/10.1016/bs.pmbts.2018.01.009
30. Jou, I., Lee, J.H., Park, S.Y., Yoon, H.J., Joe, E.H., Park, E.J.: Gangliosides trigger inflammatory responses via TLR4 in brain glia. Am. J. Pathol. **168**(5), 1619–1630 (2006). https://doi.org/10.2353/ajpath.2006.050924
31. Kawasaki, T., Kawai, T.: Toll-like receptor signaling pathways. Front. Immunol. **5**, 461 (2014). https://doi.org/10.3389/fimmu.2014.00461
32. Amith, S.R., Jayanth, P., Franchuk, S., Siddiqui, S., Seyrantepe, V., Gee, K., Basta, S., Beyaert, R., Pshezhetsky, A.V., Szewczuk, M.R.: Dependence of pathogen molecule-induced toll-like receptor activation and cell function on Neu1 sialidase. Glycoconj. J. **26**(9), 1197–1212 (2009). https://doi.org/10.1007/s10719-009-9239-8
33. Vitner, E.B., Platt, F.M., Futerman, A.H.: Common and uncommon pathogenic cascades in lysosomal storage diseases. J. Biol. Chem. **285**(27), 20423–20427 (2010). https://doi.org/10.1074/jbc.R110.134452
34. Bosch, M.E., Kielian, T.: Neuroinflammatory paradigms in lysosomal storage diseases. Front. Neurosci. **9**, 417 (2015). https://doi.org/10.3389/fnins.2015.00417
35. Jeyakumar, M., Thomas, R., Elliot-Smith, E., Smith, D.A., van der Spoel, A.C., d'Azzo, A., Perry, V.H., Butters, T.D., Dwek, R.A., Platt, F.M.: Central nervous system inflammation is a hallmark of pathogenesis in mouse models of GM1 and GM2 gangliosidosis. Brain **126**(Pt 4), 974–987 (2003). https://doi.org/10.1093/brain/awg089
36. Wu, G., Lu, Z.H., Kulkarni, N., Ledeen, R.W.: Deficiency of ganglioside GM1 correlates with Parkinson's disease in mice and humans. J. Neurosci. Res. **90**(10), 1997–2008 (2012). https://doi.org/10.1002/jnr.23090
37. Maglione, V., Marchi, P., Di Pardo, A., Lingrell, S., Horkey, M., Tidmarsh, E., Sipione, S.: Impaired ganglioside metabolism in Huntington's disease and neuroprotective role of GM1. The J neurosci: the official j Soc for Neurosci **30**(11), 4072–4080 (2010). https://doi.org/10.1523/JNEUROSCI.6348-09.2010
38. Magistretti, P.J., Geisler, F.H., Schneider, J.S., Li, P.A., Fiumelli, H., Sipione, S.: Gangliosides: Treatment Avenues in Neurodegenerative Disease. Front. Neurol. **10**, 859 (2019). https://doi.org/10.3389/fneur.2019.00859
39. Ariga, T., Yu, R.K.: GM1 inhibits amyloid beta-protein-induced cytokine release. Neurochem. Res. **24**(2), 219–226 (1999). https://doi.org/10.1023/a:1022557920150

40. Pan, X., De Aragão, C., Velasco-Martin, J.P., Priestman, D.A., Wu, H.Y., Takahashi, K., Yamaguchi, K., Sturiale, L., Garozzo, D., Platt, F.M., Lamarche-Vane, N., Morales, C.R., Miyagi, T., Pshezhetsky, A.V.: Neuraminidases 3 and 4 regulate neuronal function by catabolizing brain gangliosides. FASEB J. **31**(8), 3467–3483 (2017). https://doi.org/10.1096/fj.201601299R
41. Holm, M., Månsson, J.E., Vanier, M.T., Svennerholm, L.: Gangliosides of human, bovine and rabbit retina. Biochem. Biophys. Acta. **280**(2), 356–364 (1972). https://doi.org/10.1016/0005-2760(72)90104-x
42. Kyrkanides, S., Miller, A.W., Miller, J.N., Tallents, R.H., Brouxhon, S.M., Olschowka, M.E., O'Banion, M.K., Olschowka, J.A.: Peripheral blood mononuclear cell infiltration and neuroinflammation in the HexB-/- mouse model of neurodegeneration. J. Neuroimmunol. **203**(1), 50–57 (2008). https://doi.org/10.1016/j.jneuroim.2008.06.024
43. Domingues, H.S., Portugal, C.C., Socodato, R., Relvas, J.B.: Oligodendrocyte, Astrocyte, and Microglia Crosstalk in Myelin Development, Damage, and Repair. Frontiers in Cell and Developmental Biology **4**, 71 (2016). https://doi.org/10.3389/fcell.2016.00071
44. di Penta, A., Moreno, B., Reix, S., Fernandez-Diez, B., Villanueva, M., Errea, O., Escala, N., Vandenbroeck, K., Comella, J.X., Villoslada, P.: Oxidative stress and proinflammatory cytokines contribute to demyelination and axonal damage in a cerebellar culture model of neuroinflammation. PLoS One **8**(2), e54722 (2013). https://doi.org/10.1371/journal.pone.0054722
45. Sandhoff, K., Harzer, K.: Gangliosides and gangliosidoses: principles of molecular and metabolic pathogenesis. J. Neurosci. **33**(25), 10195–10208 (2013). https://doi.org/10.1523/JNEUROSCI.0822-13.2013
46. Kolter, T., Doering, T., Wilkening, G., Werth, N., Sandhoff, K.: Recent advances in the biochemistry of glycosphingolipid metabolism. Biochem. Soc. Trans. **27**(4), 409–415 (1999). https://doi.org/10.1042/bst0270409
47. Xu, Y.H., Barnes, S., Sun, Y., Grabowski, G.A.: Multi-system disorders of glycosphingolipid and ganglioside metabolism. J. Lipid Res. **51**(7), 1643–1675 (2010). https://doi.org/10.1194/jlr.R003996
48. Zhang, J.M., An, J.: Cytokines, inflammation, and pain. Int. Anesthesiol. Clin. **45**(2), 27–37 (2007). https://doi.org/10.1097/AIA.0b013e318034194e
49. Reichel, C.A., Rehberg, M., Lerchenberger, M., Berberich, N., Bihari, P., Khandoga, A.G., Zahler, S., Krombach, F.: Ccl2 and Ccl3 mediate neutrophil recruitment via induction of protein synthesis and generation of lipid mediators. Arterioscler. Thromb. Vasc. Biol. **29**(11), 1787–1793 (2009). https://doi.org/10.1161/ATVBAHA.109.193268
50. Marshall, A., Celentano, A., Cirillo, N., McCullough, M., Porter, S.: Tissue-specific regulation of CXCL9/10/11 chemokines in keratinocytes: Implications for oral inflammatory disease. PLoS One **12**(3), e0172821 (2017). https://doi.org/10.1371/journal.pone.0172821
51. Finlay, T.M., Abdulkhalek, S., Gilmour, A., Guzzo, C., Jayanth, P., Amith, S.R., Gee, K., Beyaert, R., Szewczuk, M.R.: Thymoquinone-induced Neu4 sialidase activates NFκB in macrophage cells and pro-inflammatory cytokines *in vivo*. Glycoconj. J. **27**(6), 583–600 (2010). https://doi.org/10.1007/s10719-010-9302-5
52. Wang, Y., Cui, Y., Cao, F., Qin, Y., Li, W., & Zhang, J.: Ganglioside GD1a suppresses LPS-induced pro-inflammatory cytokines in RAW264.7 macrophages by reducing MAPKs and NF-κB signaling pathways through TLR4. Int Immunopharmacol **28**(1), 136–145 (2015). https://doi.org/10.1016/j.intimp.2015.05.044
53. Nikolaeva, S., Bayunova, L., Sokolova, T., Vlasova, Y., Bachteeva, V., Avrova, N., & Parnova, R.: GM1 and GD1a gangliosides modulate toxic and inflammatory effects of E. coli lipopolysaccharide by preventing TLR4 translocation into lipid rafts. Biochimica et Biophysica Acta **1851**(3), 239–247 (2015). https://doi.org/10.1016/j.bbalip.2014.12.004
54. Horwood, N.J., Urbaniak, A.M., Danks, L.: Tec family kinases in inflammation and disease. Int. Rev. Immunol. **31**(2), 87–103 (2012). https://doi.org/10.3109/08830185.2012.670334
55. Ní Gabhann, J., Hams, E., Smith, S., Wynne, C., Byrne, J.C., Brennan, K., Spence, S., Kissenpfennig, A., Johnston, J.A., Fallon, P.G., Jefferies, C.A.: Btk regulates macrophage polarization in response to lipopolysaccharide. PLoS One **9**(1), e85834 (2014). https://doi.org/10.1371/journal.pone.0085834
56. Di Virgilio, F.: New pathways for reactive oxygen species generation in inflammation and potential novel pharmacological targets. Curr. Pharm. Des. **10**(14), 1647–1652 (2004). https://doi.org/10.2174/1381612043384727
57. Minami A., Saito M., Mamada S., Ieno D., Hikita T., Takahashi T., Otsubo T., Ikeda K., Suzuki T. (2016). Role of Sialidase in Long-Term Potentiation at Mossy Fiber-CA3 Synapses and Hippocampus-Dependent Spatial Memory. PLoS One. Oct 26;**11**(10), e0165257